mathematics

Article

Perception of Facial Impressions Using Explicit Features of the Face (xFoFs)

Jihyeon Yeom [1], Jeongin Lee [1], Heekyung Yang [2,*,†] and Kyungha Min [1,*,†]

[1] Department of Computer Science, Sangmyung University, 20, Hongjimun 2-gil, Jongno-gu, Seoul 03016, Republic of Korea; jihyunyum@smu.ac.kr (J.Y.); junginlee@smu.ac.kr (J.L.)
[2] Department of Software, Sangmyung University, 31, Sangmyeongdae-gil, Dongnam-gu, Cheonan 31066, Republic of Korea
[*] Correspondence: yanghk@smu.ac.kr (H.Y.); minkh@smu.ac.kr (K.M.); Tel.: +82-2-2287-6156 (H.Y.); +82-2-2287-5377 (K.M.)
[†] These authors contributed equally to this work.

Abstract: We present a novel approach to perceiving facial impressions by defining the explicit features of the face (xFoFs) based on anthropometric studies. The xFoFs estimate 35 anthropometric features of human faces with normal expressions and frontalized poses. Using these xFoFs, we have developed a method to objectively measure facial impressions, compiling a dataset of approximately 4896 facial images to validate our method. The ranking of xFoFs among the face image dataset guides an objective and quantitative estimation of facial impressions. To further corroborate our study, we conducted two user studies: an examination of the first and strongest impression perception and a validation of the consistency of multiple important impression perceptions. Our work significantly contributes to the field of facial recognition and explainable artificial intelligence (XAI) by providing an effective solution for integrating xFoFs with existing facial recognition models.

Keywords: facial features; face recognition; explainable AI; anthropometry

MSC: 62R07

Citation: Yeom, J.; Lee, J.; Yang, H.; Min, K. Perception of Facial Impressions Using Explicit Features of the Face (xFoFs). *Mathematics* **2023**, *11*, 3779. https://doi.org/10.3390/math11173779

Academic Editor: Junlin Hu

Received: 10 July 2023
Revised: 18 August 2023
Accepted: 21 August 2023
Published: 3 September 2023

1. Introduction

As humans interact with one another, they receive a multitude of sensory inputs that coalesce to form a holistic impression of the other individual. One key component of this impression comes from the facial appearance of a person. We denote a facial impression as the mental image of a person, which is primarily derived from the most distinctive facial features recognized and subsequently remembered. However, since these impressions are highly subjective, it is challenging to explicitly express them due to their inherent subjectivity. For instance, if an observer perceives an individual as having large eyes, other observers may not concur with this assessment. Furthermore, providing an objective description of the shape of an individual's face is a complex task. This is compounded by the difficulty of forming clear and objective facial impressions of individuals with ordinary facial features. Therefore, it remains a significant challenge to express facial impressions of individuals in an objective and quantitative way.

We propose a framework for perceiving facial impressions in a quantitative and objective way. The first challenge of our framework is to define the overall facial features in a quantitative way and extract them properly. Many existing studies extracted facial features using landmark points, the discretized approximation of the boundaries of important face components. However, they showed limitations in extracting correct facial features, since the landmark is an approximation of the correct boundaries of facial components. The diverse poses of a face may cause incorrect features, since the landmarks from the faces inclining to the left or right side become inconsistent. We resolve these limitations by employing deep learning-based background techniques that frontalize faces of diverse poses [1], segment important facial components [2] and align facial landmarks [3]. Based on anthropometry studies, we define 35 explicit and explainable facial features (i.e., explicit features of faces (xFoFs)) that capture the critical aspects of facial morphology using segmented regions and landmark points.

The second challenge of our framework is how to perceive facial impressions in a quantitative and objective way. We employ xFoFs for perceiving facial impressions. We denote that the ranking of xFoFs plays a key role in perceiving facial impressions. Therefore, we curate a dataset of 4896 facial images and estimate the xFoFs for each face in the dataset. The distinctive impression of an individual's face is denoted as the ranking of the corresponding xFoF of the individual's face. For example, the 17th xFoF denotes the ratio of the eye area to the face area. Therefore, a face whose 17th xFoF's ranking is high is identified to have big eyes, and a face whose 17th xFoF's ranking is low is identified to have small eyes. Our framework identifies a face with highly ranked or low-ranked xFoFs as a face whose impression is distinctive. This approach presents a quantitative and objective estimation of face impressions, which have hardly been studied by the existing approaches.

The third challenge is how to prove that our framework perceives impressions correctly. We claim the perception of a facial impression should be examined for two aspects. The first aspect regards the first and strongest impression, and the second aspect is about multiple important impressions. Therefore, we designed two distinctive user studies. In the first user study, the first impression perceived by our framework is compared to the first impression recognized by human participants. The similarity of the perceived and recognized first impressions shows that our framework successfully perceives the first impression from face images. In the second user study, the distribution of multiple important impressions perceived by our framework is compared to that recognized by the human participants. The similarity of the distributions shows that our framework successfully perceives multiple important impressions from face images.

This study makes several significant contributions to the field of facial expression recognition, which can be summarized as follows:

(1) The existing anthropometric studies defined and extracted only restricted sets of facial features. We define a set of explicit and explainable facial features (xFoFs) for the overall facial components from 68 facial landmark points and present robust extraction schemes for xFoFs using deep learning-based background techniques.
(2) Since impressions from human faces are recognized as subjective and qualitative, few studies have attacked the problem of measuring facial impressions. For an objective and quantitative estimation of facial impressions, we present a scheme that measures the rankings of the xFoFs of an individual face from the faces in a dataset. A face with high- or low-ranking xFoFs is distinguished to possess recognizable facial impressions.
(3) A challenge in this study is how to prove that the facial impressions perceived by our framework are correct. To overcome this challenge, we design two user studies: one study to prove the first and strongest impression perceived by our study is correct and another study to prove that multiple important facial impressions perceived by our framework correspond to those recognized by humans. This pair of user studies can be employed for other studies on facial feature recognition.

2. Related Work

2.1. Anthropometrical Facial Feature Measurements

Farkas [4] presented a fundamental study for an anthropometrical approach to facial features that measures the head and face anthropometric features, including angles, distances and proportions. He also investigated several derived features such as facial asymmetry, gender differences and related facial changes. Vegter and Hage [5] compared modern clinical anthropometric methods with traditional human facial measurement methods that have been employed since ancient Greek times. They analyzed the effects of the ancient golden ratio, the standards of Renaissance artists, body anthropology and cephalometry on modern facial anthropometry. They also investigated how anthropometry methods evolved from the traditional methods.

Merler et al. [6] presented a method for measuring diversity in a data-dependent face recognition model in order to verify that the data on a human face contain sufficient information for the recognition model. First, they extracted landmarks from the detected faces and presented 10 coding schemes, including the vertical distance between face elements, proportions and facial symmetry. These coding schemes were employed for the verification of human faces. Kukharev and Kaziyeva [7] addressed the issues of morphology and shape measurement for digital facial anthropometry and presented qualitative and quantitative estimation schemes for facial features and parameters. They also investigated the relationship between facial features, genes and the attractiveness of a human. Furthermore, they designed biometric barcodes with facial measurements for analysis of the close relationship between digital facial anthropometry and the Internet of Things.

2.2. *Anthropometrical Facial Feature-Based Deep Learning Models*

Many deep learning studies employed anthropometrical facial features to enrich their models and performance.

Szlavik and Sziranyi [8] improved the performance of a face recognition model by measuring the coordinates of the nose and eyes from video using histogram and CCD methods and by extracting facial features through identification of the position of the mouth from the position of the nose.

Alrubaish and Zagrouba [9] analyzed the effects of expressions on face biometric recognition models by calculating the similarity between 22 facial feature values captured from various facial expressions. The facial feature values of neutral expressions were extracted to analyze the effects of individual facial expressions on the biometric recognition system.

Alsawwaf et al. [10] presented a scheme that measures the similarity of two human faces. For this purpose, they detected sibling landmarks, calculated landmark-based feature values and compared the similarities of two faces. Therefore, they provided quantitative numerical information on the similarities and differences of two faces.

Hong [11] presented a robust face identification scheme between two persons by extracting major landmarks in 2D and 3D face images of an identical person. The allowable range in distinguishing two persons was estimated from the distance between the mutual landmarks of the two detected images.

Ramanathan and Chellappa [12] presented a scheme that generates a human face grown from an input. They built a hypothesis that the growth of the cranial face follows a geometric invariance. From this hypothesis, they modified the growth parameters by applying a revised cardioid strain transformation. After synthesizing the face contour using the modified parameters, an age conversion model synthesized the grown face image from the frontal view of a child face image.

Sunhem and Pasupa [13] presented a feature-based recommendation model for hairstyles. Their model extracts facial features to classify faces into several facial types. This approach presents an explanation for the recommendation of hairstyles for an input face image.

Alzahrani et al. [14] presented a recommendation model that recognizes gender, face type and eyebrow type from an input face image. Their model recommends hairstyles and eyelash styles for women and hair styles for men by combining the recognized information.

Chen et al. [15] developed a recommendation system for the CelebHair dataset that inherits the properties of the CelebA dataset. They provided additional properties such as face length and proportion to the CelebHair dataset. They improved the performance of their system using the properties of the CelebHair dataset. They also proposed a try-on processing approach to try out hairstyles.

In the above studies, the anthropometric facial features not only improved the performance of the models but also presented the backgrounds for the predicted results.

2.3. Anthropometrical Facial Feature-Based Studies

The anthropometrical approach is widely used in various areas such as aesthetics, forensics and anthropology.

2.3.1. Aesthetics

Aesthetics, which studies the essence of beauty, employs anthropometrical facial features for analyzing the beauty of human faces. Liu et al. [16] employed anthropometrical facial features to measure the center line of the face that divides the left and right sides of the face and to trace the change of the center line due to facial expressions. They also measured the strength of the D face and S face to investigate left-right symmetry with quantitative values.

Little et al. [17] examined the facial features that affect facial attractiveness. Based on the features, they analyzed important causes of individual differences in face preference.

Xie et al. [18] constructed the SCUT-FBP dataset, which matches face images and their attractiveness as rated by 70 participants. They also measured 18 anthropometric feature values on the face to predict facial attractiveness with a deep learning model trained by their SCUT-FBP dataset.

Zheng et al. [19] presented a mathematical model of facial proportions to explain the attractiveness of faces in a quantitative way and proved that there are statistical differences according to gender and race.

Wei et al. [20] implemented an application that predicted facial beauty scores by measuring the anthropometric feature values from facial landmarks using the Google Face API. They also presented a model that predicted perceived attractiveness based on their feature values.

2.3.2. Forensics

Roelofse et al. [21] analyzed 13 measurements and 8 morphological features in the frontal facial photographs of 100 volunteers to determine common and rare facial features that could be observed in a South African male group.

Moreton [22] discussed the various ways in which face identification can be presented as evidence in British court. He also demonstrated the scientific validity of the process used for forensic matching. Finally, he presented simulated examples that show how face identification is demonstrated.

Verma et al. [23] measured the ratios and distances of the landmarks extracted from face images and conducted a study on estimating gender from face images using logistic regression and likelihood ratio approaches with corresponding feature values. They devised a face recognition scheme by defining 11 distances and ratios from the facial feature values. Finally, they presented a new approach using a likelihood ratio based on the feature values.

Sezgin and Karadayi [24] defined 11 anthropometric values from the face images and conducted a study to estimate the gender of the Turkish population based on the anthropometric values using a statistical analysis method.

2.3.3. Anthropology

Anthropology is the science of human beings and culture aiming to comprehend human beings from cultural and biological aspects. Therefore, anthropometrical facial features play an important role in anthropology.

Porter and Olson [25] analyzed the differences between African American and Caucasian women. For this purpose, they measured the horizontal and vertical distances and proportions of the face and evaluated the differences in facial proportions between these two groups through a statistical analysis process.

Farkas et al. [26] analyzed the significant differences between races by obtaining the facial measurements of 1470 people. They constructed a craniofacial database based on accurate anthropometric measurements. They proved that their approach contributes a successful cure to congenital or post-traumatic facial deformities. Zhuang et al. [27]

designed a respirator from the data measured from 3997 US civilian workers. They analyzed the differences in facial shape and size between racial and age groups from the samples.

Packiriswamy et al. [28] quantified the size and position of the eyebrows and eyelids in two groups from standardized photographs of 200 South Indians and 200 Malaysian South Indians. They also measured whether there were significant differences between genders and ethnicities.

Maalman et al. [29] examined the vertical length of a face and a forehead. By measuring anthropometric feature values such as length, they found that there were large differences in 6 out of 10 features between the compared tribes.

3. Overview

Figure 1 depicts our framework for quantitatively measuring and extracting impressions from human faces using xFoFs. We define xFoFs by categorizing a human face into components such as the eyes, eyebrows, facial shape, nose, lips, eyelid, glabella, forehead, philtrum and chin and then devise a series of formulas to measure the xFoFs from each component. Based on these formulas, each xFoF is extracted from preprocessed face photographs. Additionally, we estimate the impression of an input face by measuring the ranking of the xFoF based on the xFoFs obtained from the faces in the face database. To validate our estimated impression, we conduct a pair of user studies to collect the impressions of a face from the participants, and we validate the results of this study by comparing them with the xFoF ranking-based impressions obtained in this study.

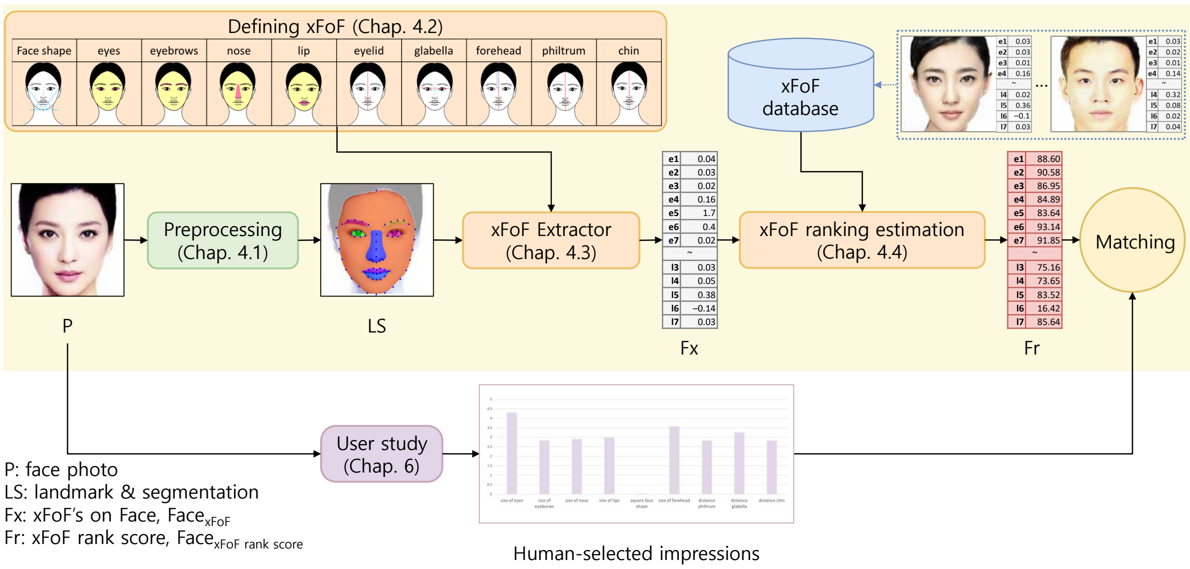

Figure 1. The overview of our approach.

4. Method

4.1. Preprocessing

Our framework assumes that the input face is hedcut and frontal. However, the face images collected in this study consisted not only of frontal hedcut images but also side or upper-body images. To achieve consistent results from the diverse poses of the face images, we converted them to front hedcut face images in the preprocessing stage. To this end, we employed Zhou et al.'s frontalization algorithm [1] to transform the face images of different poses into front hedcut face images.

The xFoFs estimated from the face images were defined based on the landmark and region information of the face. Hence, we segmented the face into regions using Yu et al.'s segmentation algorithm [2] and located the landmarks using Dlib library [3]. The segmentation information measures the area of the facial components, while the landmarks measure the length, ratio and angle of the facial components. Specifically, we added a new landmark point at the tip of the forehead in addition to the 68 landmark points used in previous studies to define the xFoFs. Thus, we used a total of 68 landmark points to define the xFoFs.

4.2. Definition of an xFoF

To provide a quantitative measurement of a facial impression, we conducted a comprehensive review of anthropometry studies [4,6,7,9–15,18,19,23,25,28] and collected 68 facial features, eliminating any duplicates. These features are suggested in Appendix A. We classified the collected features according to their corresponding facial components and selected 25 features for inclusion in our study. We then applied a rigorous process to investigate the correlation between these features and merged those with a correlation value of 0.7 or higher, following the methodology suggested by Dancey and Reidy [30]. Additionally, to capture the essential aspects of a facial impression not covered by the collected features, we identified and defined 10 new features. As a result, our study defines a total of 35 xFoFs, including 4 for the facial shape, 4 for eyebrows, 9 for eyes, 5 for the nose, 7 for lips, 2 for the chin, 1 for the forehead, 1 for eyelid height, 1 for inter-brow distance and 1 for the philtrum. We present the xFoFs and their formulas and references in Figures 2 and 3.

4.2.1. xFoFs for Face Shape

The 1st∼3rd xFoFs extracted from the facial features are cited in the previous research. The first xFoF quantifies the area of the face by measuring all horizontal lengths of the facial shape, while the second xFoF quantifies the length of the face by measuring the ratio of the vertical to horizontal lengths of the face. The third xFoF quantifies facial slimness by measuring the angles between the eighth point of the face and the 0th–7th and 9th–16th landmark points on the facial contour. However, these features have limitations in capturing facial features with prominent cheekbones. To address this issue, we proposed a fourth xFoF, defined as the angle between the two straight lines that make up the facial contour. The more acute the angle, the more developed the cheekbones are perceived to be, while a larger angle indicates a flatter face. This feature enabled us to determine the degree of development of not only the cheekbones but also the chin and cheeks.

4.2.2. xFoFs for Eyebrows

Among the xFoFs related to the eyebrows, the 5th xFoF, defined in previous research [28], measures the degree to which the eyebrows are raised or lowered by calculating the angle between the 17th and 20th landmark points with respect to the 21st point and the 23rd–26th landmark points with respect to the 22nd point. However, despite its utility in eyebrow shape analysis, this fifth xFoF has limitations in accurately quantifying the length, shape and thickness of the eyebrows.

To address this issue, we propose three xFoFs for eyebrow analysis. The first feature, the seventh xFoF, measures the length of the eyebrows while excluding the distance between them, which was improved upon by building upon the feature proposed by Chen et al. [15]. The second feature, the sixth xFoF, quantifies the location and degree of curvature in the eyebrows by measuring the angle between the straight lines that make up the eyebrows. Finally, the third feature, the eighth xFoF, proposes a method to quantify the thickness of the eyebrows by measuring the area of the eyebrows based on segmentation information. Our proposed xFoFs provide a more comprehensive analysis of the eyebrows, enabling improved eyebrow feature extraction for various computer vision applications.

No.	cate-gory	feature	formula	dimen-sion	refe-rence
1		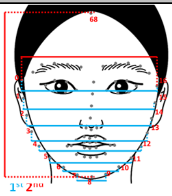	$\frac{\sum_{i=0,j=16}^{i=7,j=9} d(i,j)}{8}$	1	[Merler2019, Alrubaish2020, Alsawwaf2022, Ramanathan2006, Xie2015, Farkas2005]
2	face Shape		$\frac{d(0,16)}{d(8,68)}$	1	[Merler2019, Alrubaish2020, Alsawwaf2022, Sunhem2016]
3		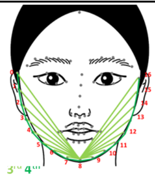	$\frac{angle(i,8)+angle(j,8)}{2}$, $i=(0,1,2,\ldots,7)$, $j=(16,15,14,\ldots,9)$	8	[Sunhem2016]
4			$\frac{angle(\overline{i,i+1},\overline{i+1,i+2})+angle(\overline{j-2,j-1},\overline{j-1,j})}{2}$, $i=(0,1,2,\ldots,6)$, $j=(16,15,14,\ldots,10)$ $angle(\overline{7,8},\overline{8\ 9})$	8	**Ours**
5		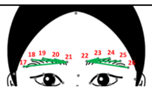	$\frac{angle(i,21)+angle(22,j)}{2}$, $i=(17,18,19,20)$, $j=(26,25,24,23)$	4	[Packiriswamy2013]
6	eye-brows	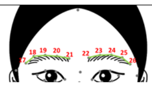	$\frac{angle(\overline{i,i+1},\overline{i+1,i+2})+angle(\overline{j-2,j-1},\overline{j-1,j})}{2}$, $i=(17,18,19)$, $j=(26,25,24)$	3	**Ours**
7		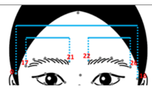	$\frac{d(17,21)+d(22,26)}{2*d(0,16)}$	1	**Ours**
8			$\frac{eyebrows\ area}{face\ area}$	1	**Ours**
9		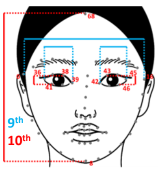	$\frac{d(36,39)+d(42,45)}{2*d(0,16)}$	1	[Vegter2000, Merler2019, Kukharev2020, Alrubaish2020, Alzahrani2021, Chen2021, Xie2015, Porter2001]
10			$\frac{d(38,41)+d(43,46)}{2*d(8,68)}$	1	[Farkas1994, Merler2019, Xie2015]
11		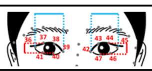	$\frac{d(\max(40,41),\min(37,38))+d(\max(46,47)-\min(43,44))}{d(36,39)+d(42,45)}$	1	[Merler2019]
12	eyes	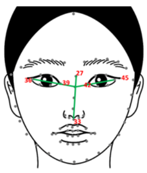	$\frac{angle(\overline{(27,33)},\overline{(36,39)})+angle(\overline{(27,33)},\overline{(42,45)})}{2}$	1	[Kukharev2020, Alzahrani2021]
13		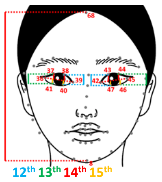	$\frac{d(38,40)+d(43,47)}{2*d(8,68)}$	1	[Alzahrani2021]
14			$\frac{d(37,41)+d(44,46)}{2*d(8,68)}$	1	[Alzahrani2021, Packiriswamy2013]
15			$\frac{d(\overline{36,39},37)+d(\overline{36,39},38)+d(\overline{42\ 45},43),d(\overline{42\ 45},44)}{4*d(8,68)}$	1	**Ours**
16			$\frac{d(\overline{36,39},40)+d(\overline{36,39},41)+d(\overline{42\ 45},46),d(\overline{42\ 45},47)}{4*d(8,68)}$	1	**Ours**
17			$\frac{eyes\ area}{face\ area}$	1	**Ours**

Figure 2. The xFoFs and their formulas (0th∼17th xFoFs).

No.	category	feature	formula	dimension	reference
18	nose	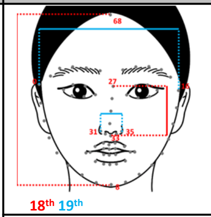	$\frac{d(27,33)}{d(8,68)}$	1	[Merler2019, Kukharev2020, Alrubaish2020, Alsawwaf2022, Chen2021, Xie2015, Zheng2022, Porter2001, Farkas2005]
19			$\frac{d(31,35)}{d(0,16)}$	1	[Vegter2000, Merler2019, Xie2015, Zheng2022, Porter2001]
20		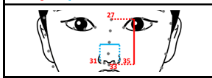	$\frac{d(31,35)}{d(27,33)}$	1	[Merler2019, Alrubaish2020]
21		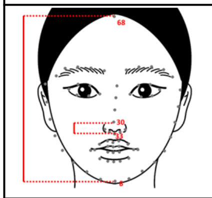	$\frac{d(30,33)}{d(8,68)}$	1	[Merler2019]
22			$\frac{nose\ area}{face\ area}$	1	**Ours**
23	lip	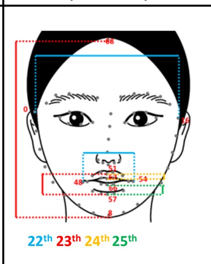	$\frac{d(48,54)}{d(0,16)}$	1	[Vegter2000, Merler2019, Kukharev2020, Alrubaish2020, Xie2015, Porter2001, Farkas2005]
24			$\frac{d(51,57)}{d(8,68)}$	1	[Vegter2000, Merler2019]
25			$\frac{d(51,62)}{d(8,68)}$	1	[Vegter2000, Merler2019]
26			$\frac{d(57,66)}{d(8,68)}$	1	[Vegter2000, Merler2019]
27		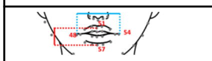	$\frac{d(51,57)}{d(48,54)}$	1	[Merler2019]
28		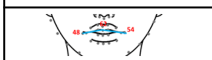	$\frac{angle(48,62)+angle(54,62)}{2}$	**1**	**Ours**
29		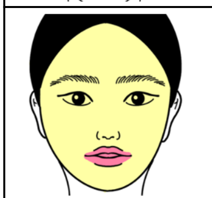	$\frac{lip\ area}{face\ area}$	1	**Ours**
30	forehead	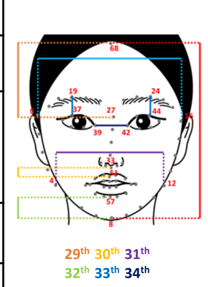	$\frac{d(27,68)}{d(8,68)}$	1	[Vegter2000, Merler2019, Porter2001, Farkas2005]
31	philtrum		$\frac{d(33,51)}{d(8,68)}$	1	[Farkas1994, Merler2019, Xie2015]
32	chin		$\frac{d(4,12)}{d(0,16)}$	1	[Xie2015]
33			$\frac{d(8,57)}{d(8,68)}$	**1**	[Vegter2000, Merler2019]
34	eyelid		$\frac{d(19,37)+d(24,44)}{2*d(8,68)}$	1	[Xie2015, Packiriswamy2013]
35	glabella		$\frac{d(39,42)}{d(0,16)}$	1	[Merler2019,Alsawwaf2022,Ramanathan2006, Alzahrani2021, Xie2015,Zheng2022, Porter2001, Farkas2005]

Figure 3. The xFoFs and their formulas (18th∼35th xFoFs).

4.2.3. xFoFs for the Eyes

Among the xFoFs that describe an eye, we identified the 9th∼14th xFoFs from previous studies. The 9th xFoF measures the horizontal length of the eye, while the 10th xFoF measures its vertical length. The 11th xFoF measures the ratio of the width to the height of the eye to determine whether the eye is thin like a narrow eye. The 12th xFoF measures the angle of the eye tail, quantifying how much the eye tail rises or falls. The 13th and 14th xFoFs measure the vertical lengths of the front and back of the eye, respectively, and quantitatively express the degree to which the eye increases or decreases in size toward the end. While these xFoFs are useful for characterizing the eye, they have limitations in measuring the curvature and size of the eye.

To address these limitations, we propose two new xFoFs. First, we define the 15th and 16th xFoFs to measure the roundness of the upper and lower lines of the eye by measuring the curvature of the upper and lower curves of the eye, respectively. This measure provides additional information on the shape of the eye that is not captured by the existing xFoFs. Secondly, we define the 17th xFoF to measure the area of the eye based on segmentation information. This measure complements the information on the shape of the eye by providing a measure of the eye's size.

4.2.4. xFoFs for the Nose

Among the xFoFs defined for the nose, we defined the 18th$\sim$22th xFoFs based on the features presented in earlier studies. The 18th xFoF measures the vertical length of the nose, while the 19th xFoF measures its horizontal length. The 20th xFoF quantifies whether the nose is round or long by measuring the ratio of the vertical length to the horizontal length of the nose. The 21st xFoF quantifies the size of the nostrils when viewed from the front by measuring the distance between the 30th and 31st landmark points. These xFoFs effectively capture the morphological characteristics of the nose, but they have limited ability to measure the size of the nose. In this study, we introduce the 22nd xFoF, which characterizes the area of the nose based on segmentation information to provide a more accurate measurement of the nose's size.

4.2.5. xFoFs for the Lips

The 23rd and 24th xFoFs for the lips are defined based on features from earlier studies, where they measure the horizontal and vertical lengths of the lips, respectively. The 25th xFoF quantifies the thickness of the upper lip by measuring its vertical length, while the 26th one quantifies the thickness of the lower lip by measuring its vertical length. The 27th xFoF quantifies whether the lips are round or long by measuring the ratio of the horizontal length to the vertical length of the lips. However, these xFoFs have limitations in accurately representing the overall shape of the lips.

In this paper, we introduce two new xFoFs to better quantify the lip features. First, the 28th xFoF measures the degree to which the angle of the lip corners is raised or lowered relative to the midpoint of the lips. This new feature is expected to provide a more complete and precise understanding of the shape of the lips. Secondly, we suggest the 29th xFoF, which characterizes the area of the lips based on segmentation information, thereby offering a more objective quantification of lip size.

4.2.6. xFoFs for Other Features

We defined the xFoFs for various facial components, including the forehead, glabella, philtrum, upper eyelid height and chin, based on previous research. Specifically, the width of the forehead is measured using the 30th xFoF. The 31st xFoF is used to express the length of the glabella. The 32nd and 33rd xFoFs are used to define the horizontal and vertical lengths of the chin, respectively. The height of the upper eyelid, defined as the distance between the eyebrow and the eye, is estimated in the 34th xFoF. Lastly, the 35th xFoF is employed to measure the length of the philtrum.

4.3. Extraction of xFoFs

In the process of extracting xFoFs, the landmark and segmentation information extracted in the preprocessing stage are used as input. The xFoFs, which are defined by the formulas presented in Figures 2 and 3, measure the length, proportion, angle and area of a face. Each xFoF is extracted as a 54-dimensional vector. Note that some xFoFs are defined using multiple dimensional vectors. The extraction of xFoFs is illustrated in Figure 4.

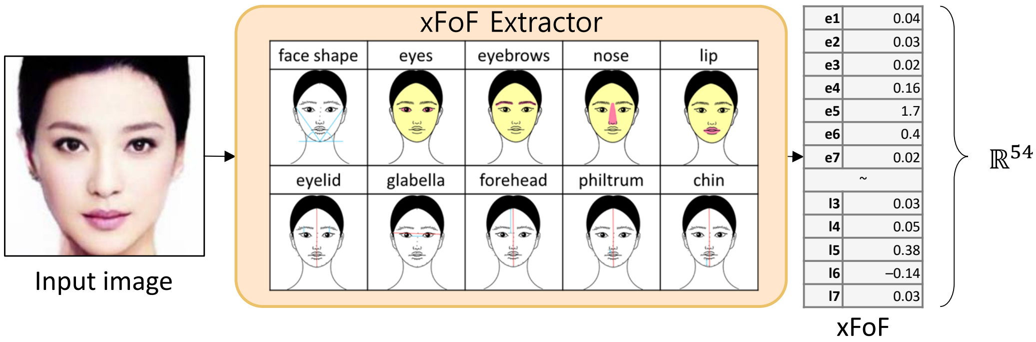

Figure 4. The extraction of xFoFs.

4.4. Estimating xFoF Rankings

The impressions of a face are generated from its relatively prominent features, and quantifying the prominence of certain components of an input face is achieved through the process of estimating the xFoF ranking. To evaluate the impression of an input face objectively, two publicly available face datasets, SCUT-FBP [18] and AFAD [31], are utilized in this research. A total of 4896 facial images were collected by excluding images with exaggerated expressions that distorted the facial identity in these two datasets. The xFoFs were extracted from the facial images in this dataset to build an xFoF database for 4896 individuals.

The xFoF ranking estimation process consists of the following steps. First, the xFoF features extracted from the input face are added to the database. Then, a t-score is calculated using a mean of 50 and a standard deviation of 10. The t-score indicates the relative prominence of a feature compared to others, taking into account the mean and standard deviation. Thus, the greater the deviation of the t-score from the mean, the higher the weight assigned to the corresponding feature, and vice versa. The weight vector is created and sorted in descending order, and the impression of the input face is quantitatively measured and represented based on the sorted weights.

Figure 5 illustrates a comparison of faces with significant t-score differences for the same xFoF component in the xFoF database. A large difference in t-scores indicates a significant difference in the ranking of the corresponding xFoF component, implying that the two faces have opposite features. This figure visually demonstrates that the farther the t-score values of facial components are from each other, the more opposing features they possess.

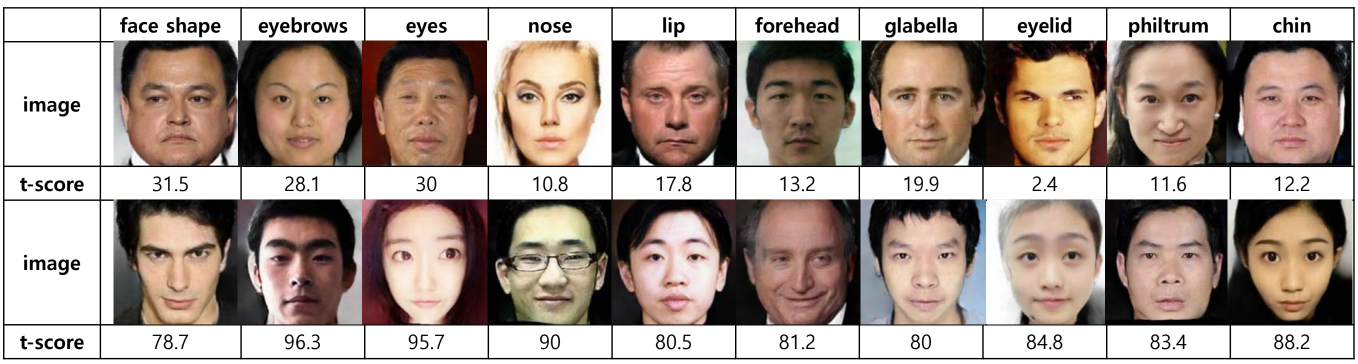

Figure 5. Pairs of faces whose t-scores have great differences.

5. Implementation and Results

5.1. Implementation

This approach was implemented on a PC with an Intel Pentium i9-9900X 3.50 GHz CPU with main memory of 128 GB and an Nvidia Titan RTX GPU. We implemented this approach using Python with the Pytorch library in the Jupyter notebook environment. We employed Pandas for the manipulation of the xFoF database. Landmark detection was implemented using the Dlib library [3]. Semantic segmentation and frontalization were implemented using Gao et al.'s work [2] and Zhou et al.'s work [1], respectively. The face image dataset we employed was AFAD [31] and SCUT-FBP [18].

The deep learning models [1–3] in this study were the pretrained models, which did not require further training.

5.2. Results

In order to normalize and compare the xFoF rankings, we estimated the t-scores from the xFoF distribution and their corresponding percentages using the following approach:

(1) For each set of xFoFs extracted from a dataset of 4896 faces, we calculated the mean and standard deviation of each xFoF distribution and computed the t-scores from the values [32].
(2) The xFoF ranking for a prominent impression may be very high or very low, indicating that an xFoF with a large or small t-score value is an important feature for a face. For example, a face with very large eyes would have a high t-score for an xFoF related to the eye size, while a face with very small eyes would have a small t-score for the same xFoF. Faces with very large or very small eyes can both be classified as having prominent impressions.
(3) The percentage that each feature belongs to a certain interval of t-scores can be used as a measure of the likelihood that the feature is a prominent one. Using the percentage of belonging to an interval of t-scores as a quantitative indicator of features is much more effective than using the t-score alone. For example, if the t-score for very large eyes is 99, and the t-score for very small eyes is 1, although there is a large difference between them, both are located at the extremes of the distribution and can be considered to belong to the percentage of 0.13%. Therefore, we divide the t-scores into appropriate percentages and calculate the percentages of each interval as follows [32].
(4) The percentage of t-scores falling into the intervals 0∼20 and 80∼100 is 0.13% each, the percentage of t-scores falling into the intervals 20∼30 and 70∼80 is 2.14% each, the percentage of t-scores falling into the intervals 30∼40 and 60∼70 is 13.59% each, and the percentage of t-scores falling into the interval 40∼60 is 68.26% [32]. This process is illustrated in Figure 6.
(5) All xFoFs can be classified according to facial components, and the rankings of the extracted xFoFs can be organized as shown in Figure 7.

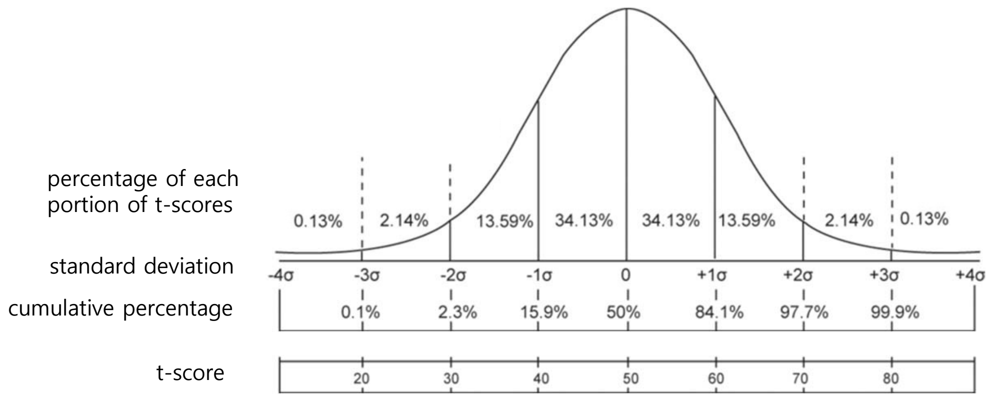

Figure 6. The t-scores and the percentage of each portion of t-scores.

component	xFoF	0 ~ 20 (under 0.1%)	20 ~ 30 (0.1~2.3%)	30 ~ 40 (2.3~15.9%)	40 ~ 50 (15.9~50%)	50 ~ 60 (50~84.1%)	60 ~ 70 (84.1~97.7%)	70 ~ 80 (97.7%)	80 ~ 100 (over 99.9%)	total
face shape	1	15	128	624	1,607	1,764	673	83	2	4,896
	2	7	114	634	1,722	1,667	631	111	10	4,896
	3	0	9	761	1,960	1,349	611	189	17	4,896
	3	0	14	792	1,849	1,348	733	154	6	4,896
	3	0	43	794	1,756	1,401	777	125	0	4,896
	3	0	64	769	1,735	1,433	790	105	0	4,896
	3	0	62	768	1,724	1,454	790	98	0	4,896
	3	0	43	789	1,736	1,448	764	116	0	4,896
	3	0	21	770	1,863	1,355	720	165	2	4,896
	3	0	32	692	2,001	1,354	619	183	15	4,896
	4	5	88	627	1,819	1,568	542	247	0	4,896
	4	16	143	631	1,544	1,768	794	0	0	4,896
	4	11	110	643	1,707	1,645	667	106	7	4,896
	4	9	113	647	1,665	1,713	635	110	4	4,896
	4	2	122	670	1,635	1,716	626	122	3	4,896
	4	3	63	739	1,711	1,585	649	139	7	4,896
	4	5	89	727	1,587	1,633	796	59	0	4,896
	4	40	227	484	1,234	2,344	567	0	0	4,896
eyebrow	5	9	120	672	1,559	1,766	676	91	3	4,896
	5	3	115	694	1,593	1,710	678	100	3	4,896
	5	4	99	670	1,700	1,640	662	110	11	4,896
	5	6	85	638	1,744	1,668	620	124	11	4,896
	6	4	87	689	1,713	1,627	662	110	4	4,896
	6	11	126	640	1,636	1,708	687	84	4	4,896
	6	9	124	639	1,662	1,674	694	88	6	4,896
	7	4	93	683	1,703	1,622	675	107	9	4,896
	8	4	62	699	1,765	1,621	611	109	25	4,896
eye	9	0	34	679	1,993	1,474	508	168	40	4,896
	10	4	95	684	1,712	1,655	620	113	13	4,896
	11	7	97	672	1,668	1,656	682	111	3	4,896
	12	2	69	707	1,804	1,491	686	134	3	4,896
	13	2	81	682	1,790	1,588	599	137	17	4,896
	14	3	86	709	1,720	1,608	633	125	12	4,896
	15	5	80	687	1,752	1,616	621	122	13	4,896
	16	2	76	654	1,808	1,595	610	130	21	4,896
	17	0	15	675	2,052	1,417	532	158	47	4,896
nose	18	0	52	645	1,925	1,524	555	161	34	4,896
	19	2	76	674	1,789	1,598	611	122	24	4,896
	20	1	77	738	1,700	1,602	644	120	14	4,896
	21	7	143	646	1,567	1,811	629	89	4	4,896
	22	0	58	653	1,921	1,540	537	155	32	4,896
lip	23	1	56	714	1,796	1,568	594	148	19	4,896
	24	12	108	626	1,697	1,721	606	114	12	4,896
	25	2	134	641	1,552	1,754	723	85	5	4,896
	26	18	130	587	1,643	1,782	637	92	7	4,896
	27	7	104	634	1,739	1,663	619	121	9	4,896
	28	19	155	617	1,459	1,905	686	54	1	4,896
	29	4	93	666	1,714	1,651	646	109	13	4,896
forehead	30	18	88	581	1,823	1,706	524	132	24	4,896
philtrum	31	13	112	635	1,642	1,722	681	84	7	4,896
chin	32	32	159	504	1,620	1,889	600	91	1	4,896
chin	33	37	163	504	1,549	1,959	631	52	1	4,896
eyelid	34	53	133	476	1,629	1,912	636	54	3	4,896
glabella	35	2	88	680	1,709	1,662	621	120	14	4,896
Total		**420**	**4,958**	**35,955**	**92,703**	**88,650**	**35,020**	**6,136**	**542**	**26,4384**
percentage		**0.159%**	**1.875%**	**13.600%**	**35.064%**	**33.531%**	**13.246%**	**2.321%**	**0.205%**	**100%**

Figure 7. The xFoF rankings by t-scores.

6. Evaluation

6.1. First User Study on Catching Dominant Impressions

The primary aim of the first user study was to assess the efficacy of xFoF ranking in identifying the impressions perceived by the participants. We denoted the impression as a facial component that is recognized primarily by the participants. For this study, we recruited a sample of 30 participants, 24 of whom were in their 20s and 6 of whom were in their 30s, comprising 17 males and 13 females. Of these participants, 19 were undergraduate students, and 11 were graduate students.

To conduct the study, we selected a representative sample of 30 facial images from our dataset, which comprises a total of 4896 images.

6.1.1. Results of First User Study on Catching Dominant Impressions

In order to assess the participants' perceptions of dominant impressions for various facial components, they were asked to assign a clear ranking to each of the 10 components: facial shape, eyes, eyebrows, nose, mouth, chin, eyelid, glabella, philtrum and forehead. This ranking system utilized a 10-point scale, with a score of 10 indicating the component with the most dominant impression and a score of 1 indicating the component with the least dominant impression.

Figures 8–10 present the results of the user study for 10 faces. Each face was divided into two rows: the top row displayed the average values of the face components rated by 30 participants using a 10-point metric (1–10). The component perceived as the most dominant impression is shown in the leftmost column, while the component perceived as the least dominant impression is shown in the rightmost column. Each cell shows the average score and the corresponding component.

The bottom row displays the 10 components sorted in descending order of their xFoF ranking percentages. Each cell shows the xFoF ranking and its corresponding percentage of the t-score. The xFoF ranking indicates how distinct a component was perceived to be, with values closer to the ends of the scale indicating higher distinctiveness. The value within parentheses indicates the probability of the t-score belonging to that interval. For example, if the xFoF value for the face shape component in the leftmost column of the first face is 4895, then it is a significant value, and the percentage belonging to the 80∼100 interval of the t-score is 0.13%.

The components that received the top rank in the user study are highlighted in bold in the table. Thus, the bold figures in the bottom row of each face indicate the component that was ranked first in the user study. For instance, the first and second faces show that the feature that was ranked first in the user study was also ranked first in the xFoF ranking. However, for the third face, the feature that was ranked first in the user study was ranked second in the xFoF ranking.

These tables highlight components based on their corresponding t-scores in the xFoF ranking. Specifically, dark orange cells denote components with a t-score falling in the 0.13% range, orange cells denote t-scores in the 2.14% range, and light orange cells indicate t-scores in the 13.59% range. Note that the distribution of highlighted cells varied across the different faces due to the different xFoF ranking distributions. Faces with more dark orange cells indicate more distinctive components, while faces with fewer orange cells suggest more typical components.

No.	image	score	1	2	3	4	5	6	7	8	9	10
1		user study mean score	**face shape 9.9**	nose 7.7	eye 7.65	lip 6.5	forehead 5.35	eyebrow 5.05	chin 3.9	eyelid 3.4	glabella 2.85	philtrum 2.7
		rank (percentage)	**face shape 4895 (0.13)**	eye 98 (2.14)	glabella 171 (13.59)	eyebrow 4400 (13.59)	lip 4450 (13.59)	nose 819 (34.13)	chin 3003 (34.13)	eyelid 2875 (34.13)	forehead 2620 (34.13)	philtrum 2345 (34.13)
2		user study mean score	**face shape 8.7**	eyebrow 8.65	lip 6.25	eye 5.9	forehead 5.9	glabella 4.85	nose 4.45	philtrum 4.4	chin 3.15	eyelid 2.75
		rank (percentage)	**face shape 4868 (2.14)**	eyebrow 75 (2.14)	glabella 104 (13.59)	nose 63 (13.59)	lip 4471 (13.59)	forehead 4427 (13.59)	eye 811 (34.13)	philtrum 860 (34.13)	chin 3527 (34.13)	eyelid 2845 (34.13)
3		user study mean score	**eye 9.3**	face shape 7.45	nose 7.1	lip 6.35	forehead 6.15	eyebrow 5.75	eyelid 3.85	glabella 3.35	philtrum 2.9	chin 2.8
		rank (percentage)	face shape 67 (2.14)	**eye 4596 (13.59)**	nose 195 (13.59)	eyebrow 4492 (13.59)	eyelid 682 (34.13)	lip 797 (34.13)	glabella 1340 (34.13)	chin 3287 (34.13)	philtrum 2893 (34.13)	forehead 2525 (34.13)
4		user study mean score	**eye 7.75**	nose 7.0	face shape 6.95	forehead 6.65	eyebrow 6.4	lip 5.7	philtrum 4.5	glabella 4.3	eyelid 3.5	chin 2.25
		rank (percentage)	face shape 4495 (13.59)	eyebrow 352 (13.59)	**eye 4227 (13.59)**	lip 1041 (34.13)	forehead 3884 (34.13)	nose 3741 (34.13)	eyelid 2907 (34.13)	glabella 2261 (34.13)	philtrum 2582 (34.13)	chin 2319 (34.13)
5		user study mean score	**eyebrow 7.9**	eyelid 7.2	face shape 7.0	lip 5.75	chin 5.45	forehead 5.4	nose 5.25	eye 4.7	glabella 3.55	philtrum 2.8
		rank (percentage)	face shape 3 (0.13)	**eyebrow 10 (2.14)**	forehead 4828 (2.14)	lip 112 (2.14)	eye 4652 (13.59)	chin 290 (13.59)	nose 4425 (13.59)	eyelid 3721 (34.13)	philtrum 1513 (34.13)	glabella 3315 (34.13)
6		user study mean score	**nose 9.4**	eye 9.0	face shape 6.9	lip 6.1	eyebrow 5.55	forehead 4.5	glabella 4.35	eyelid 3.85	philtrum 2.7	chin 2.65
		rank (percentage)	face shape 12 (2.14)	**nose 4515 (13.59)**	lip 4443 (13.59)	eye 4165 (13.59)	glabella 3758 (34.13)	eyebrow 3616 (34.13)	forehead 1264 (34.13)	chin 3450 (34.13)	eyelid 1797 (34.13)	philtrum 1987 (34.13)
7		user study mean score	**nose 7.95**	face shape 7.85	eyebrow 6.85	forehead 6.7	eye 6.5	lip 6.25	philtrum 4.65	eyelid 3.15	glabella 3.0	chin 2.1
		rank (percentage)	face shape 4834 (2.14)	**nose 54 (2.14)**	eye 4617 (13.59)	lip 443 (13.59)	eyebrow 670 (13.59)	glabella 1137 (34.13)	forehead 3747 (34.13)	chin 1847 (34.13)	philtrum 2790 (34.13)	eyelid 2075 (34.13)
8		user study mean score	**eye 8.45**	eyelid 8.0	eyebrow 8.35	face shape 6.2	lip 5.8	nose 5.55	glabella 4.3	forehead 3.75	philtrum 2.4	chin 2.2
		rank (percentage)	face shape 50 (2.14)	lip 107 (13.59)	**eye 450 (13.59)**	eyelid 4360 (13.59)	eyebrow 788 (34.13)	forehead 4129 (34.13)	nose 3975 (34.13)	chin 1781 (34.13)	glabella 2919 (34.13)	philtrum 2399 (34.13)
9		user study mean score	**eyebrow 8.8**	eye 8.6	nose 7.8	chin 6.15	lip 4.65	forehead 4.3	face shape 4.25	eyelid 4.05	philtrum 3.8	glabella 2.6
		rank (percentage)	**eyebrow 4895 (0.13)**	face shape 4760 (13.59)	lip 174 (13.59)	eye 4506 (13.59)	nose 4484 (13.59)	chin 4416 (13.59)	philtrum 3993 (34.13)	eyelid 3581 (34.13)	glabella 1400 (34.13)	forehead 1536 (34.13)
10		user study mean score	**eyebrow 9.05**	eye 8.2	nose 7.75	lip 6.55	philtrum 4.85	eyelid 4.75	face shape 4.05	glabella 4.0	forehead 3.25	chin 2.55
		rank (percentage)	**eyebrow 7 (2.14)**	philtrum 4866 (2.14)	eye 4693 (13.59)	lip 364 (13.59)	nose 287 (13.59)	face shape 4024 (34.13)	forehead 3520 (34.13)	glabella 1804 (34.13)	eyelid 1653 (34.13)	chin 1765 (34.13)

Figure 8. The results of the user study for the first 10 face images (1∼10). Dark orange cells denote components with a t-score falling in the 0.13% range, orange cells denote t-scores in the 2.14% range, and light orange cells indicate t-scores in the 13.59% range.

No.	image	score	1	2	3	4	5	6	7	8	9	10
11		user study mean score	**eyebrow 9.55**	face shape 8.45	eyelid 6.7	chin 6.55	lip 6.0	forehead 5.95	nose 3.55	eye 3.1	glabella 2.7	philtrum 2.45
		rank (percentage)	**eyebrow 4867 (2.14)**	lip 86 (2.14)	eyelid 165 (2.14)	chin 4782 (13.59)	nose 208 (13.59)	face shape 594 (13.59)	eye 670 (13.59)	forehead 1446 (34.13)	philtrum 2554 (34.13)	glabella 2514 (34.13)
12		user study mean score	**eye 8.1**	eyebrow 7.65	face shape 7.55	lip 7.15	nose 6.6	forehead 5.6	chin 4.05	eyelid 3.35	philtrum 2.8	glabella 2.15
		rank (percentage)	eyebrow 28 (2.14)	face shape 56 (2.14)	nose 107 (13.59)	lip 606 (13.59)	chin 4336 (13.59)	**eye 886 (34.13)**	philtrum 1382 (34.13)	forehead 1643 (34.13)	glabella 2862 (34.13)	eyelid 2191 (34.13)
13		user study mean score	**eyebrow 9.6**	eye 7.1	face shape 6.2	eyelid 5.95	forehead 5.8	lip 5.1	glabella 4.6	nose 4.05	philtrum 3.8	chin 2.8
		rank (percentage)	**eyebrow 32 (2.14)**	face shape 4650 (2.14)	glabella 297 (13.59)	lip 4427 (13.59)	nose 498 (13.59)	eye 548 (13.59)	eyelid 4349 (13.59)	chin 1379 (34.13)	forehead 3219 (34.13)	philtrum 2266 (34.13)
14		user study mean score	**eyebrow 9.15**	eye 7.7	lip 7.45	nose 6.35	face shape 5.4	philtrum 4.25	eyelid 4.2	glabella 4.15	forehead 3.75	chin 2.6
		rank (percentage)	**eyebrow 29 (2.14)**	lip 4801 (2.14)	face shape 4606 (13.59)	eye 4564 (13.59)	philtrum 692 (13.59)	nose 1063 (34.13)	glabella 3286 (34.13)	eyelid 1606 (34.13)	forehead 2830 (34.13)	chin 2248 (34.13)
15		user study mean score	**face shape 8.35**	eye 8.3	nose 7.0	forehead 6.0	lip 5.75	eyebrow 5.55	glabella 4.5	eyelid 3.7	philtrum 3.4	chin 2.45
		rank (percentage)	eyebrow 222 (13.59)	**face shape 309 (13.59)**	nose 633 (13.59)	lip 4105 (13.59)	eye 1005 (34.13)	glabella 3787 (34.13)	eyelid 3468 (34.13)	philtrum 3295 (34.13)	forehead 3219 (34.13)	chin 2086 (34.13)
16		user study mean score	**eye 8.85**	face shape 8.0	forehead 7.9	lip 6.85	nose 6.35	eyebrow 5.15	philtrum 3.45	chin 3.4	eyelid 3.25	glabella 1.8
		rank (percentage)	**eye 15 (2.14)**	lip 4830 (2.14)	face shape 132 (13.59)	philtrum 200 (13.59)	nose 4549 (13.59)	eyebrow 4448 (13.59)	chin 1064 (34.13)	forehead 3570 (34.13)	glabella 3350 (34.13)	eyelid 3225 (34.13)
17		user study mean score	**eye 8.85**	lip 7.9	nose 6.95	face shape 6.25	forehead 6.15	eyelid 5.7	eyebrow 3.7	glabella 3.55	philtrum 3.5	chin 2.45
		rank (percentage)	**eye 151 (13.59)**	face shape 4369 (13.59)	lip 4501 (13.59)	eyelid 4424 (13.59)	glabella 4066 (34.13)	nose 3899 (34.13)	eyebrow 3758 (34.13)	forehead 1047 (34.13)	philtrum 3378 (34.13)	chin 1319 (34.13)
18		user study mean score	**eye 8.55**	nose 7.75	face shape 7.05	eyebrow 6.75	lip 6.05	chin 4.25	glabella 4.1	forehead 4.05	philtrum 3.7	eyelid 2.75
		rank (percentage)	**eye 4896 (0.13)**	face shape 4845 (2.14)	forehead 4718 (13.59)	lip 324 (13.59)	eyebrow 263 (13.59)	nose 410 (13.59)	chin 585 (13.59)	philtrum 667 (13.59)	glabella 3517 (34.13)	eyelid 2575 (34.13)
19		user study mean score	**eye 8.45**	eyebrow 8.4	face shape 6.5	nose 6.5	forehead 6.35	lip 5.6	eyelid 3.8	glabella 3.3	philtrum 3.1	chin 3.0
		rank (percentage)	**eye 4833 (2.14)**	nose 83 (13.59)	face shape 4530 (13.59)	lip 550 (13.59)	eyebrow 778 (13.59)	glabella 755 (13.59)	eyelid 763 (34.13)	forehead 1561 (34.13)	philtrum 2946 (34.13)	chin 2319 (34.13)
20		user study mean score	**eye 8.1**	eyebrow 7.8	face shape 7.25	lip 7.05	nose 6.45	eyelid 5.3	forehead 3.9	glabella 3.75	philtrum 2.95	chin 2.45
		rank (percentage)	**eye 4783 (2.14)**	eyebrow 199 (13.59)	face shape 259 (13.59)	lip 4566 (13.59)	nose 4172 (34.13)	glabella 1412 (34.13)	chin 3431 (34.13)	forehead 1673 (34.13)	eyelid 3013 (34.13)	philtrum 2816 (34.13)

Figure 9. The results of the user study for the second 10 face images (11∼20). Dark orange cells denote components with a t-score falling in the 0.13% range, orange cells denote t-scores in the 2.14% range, and light orange cells indicate t-scores in the 13.59% range.

No.	**image**	**score**	**1**	**2**	**3**	**4**	**5**	**6**	**7**	**8**	**9**	**10**
21		user study mean score	**eye 9.8**	nose 8.15	lip 7.15	face shape 6.35	eyebrow 6.15	chin 3.95	forehead 3.85	glabella 3.6	eyelid 3.35	philtrum 2.65
		rank (percentage)	nose 4808 (2.14)	lip 4813 (2.14)	glabella 4689 (13.59)	**eye 201 (13.59)**	eyebrow 4619 (13.59)	face shape 507 (13.59)	chin 495 (13.59)	forehead 1398 (34.13)	philtrum 2969 (34.13)	eyelid 2476 (34.13)
22		user study mean score	**nose 8.6**	eye 7.75	lip 6.15	face shape 6.1	eyebrow 5.8	philtrum 5.4	chin 4.65	forehead 4.2	glabella 3.7	eyelid 2.65
		rank (percentage)	**nose 4783 (2.14)**	eyebrow 4704 (13.59)	face shape 4678 (13.59)	philtrum 4601 (13.59)	lip 4279 (13.59)	chin 3943 (34.13)	eye 3902 (34.13)	forehead 1206 (34.13)	eyelid 1576 (34.13)	glabella 1877 (34.13)
23		user study mean score	**eye 9.65**	face shape 8.0	eyebrow 7.2	eyelid 6.3	nose 5.55	lip 5.2	philtrum 3.75	glabella 3.5	chin 3.05	forehead 2.8
		rank (percentage)	nose 41 (2.14)	eyebrow 4759 (13.59)	face shape 4650 (13.59)	**eye 4656 (13.59)**	glabella 4380 (13.59)	eyelid 536 (13.59)	lip 1183 (34.13)	chin 3323 (34.13)	forehead 3195 (34.13)	philtrum 1777 (34.13)
24		user study mean score	**lip 8.8**	face shape 8.7	nose 7.0	forehead 5.5	eye 5.2	eyebrow 4.7	glabella 4.35	eyelid 3.85	philtrum 3.85	chin 3.05
		rank (percentage)	**lip 4825 (2.14)**	face shape 4299 (13.59)	forehead 678 (13.59)	eyebrow 4110 (34.13)	nose 4050 (34.13)	eye 3941 (34.13)	glabella 3919 (34.13)	philtrum 3455 (34.13)	chin 1485 (34.13)	eyelid 2940 (34.13)
25		user study mean score	**lip 8.2**	face shape 9.0	nose 8.0	eye 6.05	eyebrow 5.3	forehead 4.55	philtrum 4.2	eyelid 3.85	glabella 3.1	chin 2.75
		rank (percentage)	**lip 4864 (2.14)**	face shape 75 (2.14)	eyelid 247 (13.59)	eye 4615 (13.59)	eyebrow 300 (13.59)	philtrum 411 (13.59)	glabella 4371 (13.59)	nose 4300 (13.59)	chin 1034 (34.13)	forehead 2462 (34.13)
26		user study mean score	**forehead 7.6**	nose 7.55	eye 6.85	lip 6.05	eyebrow 5.75	face shape 5.15	eyelid 4.95	chin 4.85	glabella 3.55	philtrum 2.7
		rank (percentage)	**forehead 4791 (2.14)**	face shape 45 (13.59)	eyebrow 212 (13.59)	nose 360 (13.59)	chin 480 (13.59)	eye 3789 (34.13)	lip 3610 (34.13)	eyelid 3031 (34.13)	glabella 1918 (34.13)	philtrum 2697 (34.13)
27		user study mean score	**philtrum 9.35**	nose 7.15	forehead 6.75	lip 6.2	eye 5.35	eyelid 5.35	face shape 4.85	glabella 4.1	eyebrow 3.75	chin 2.15
		rank (percentage)	**philtrum 1 (0.13)**	nose 4 (0.13)	forehead 4845 (2.14)	eye 4669 (13.59)	eyebrow 277 (13.59)	face shape 4404 (13.59)	lip 590 (13.59)	glabella 566 (13.59)	chin 3081 (34.13)	eyelid 2602 (34.13)
28		user study mean score	**face shape 8.8**	eye 8.75	eyebrow 6.5	nose 6.4	glabella 5.65	chin 5.0	lip 4.45	philtrum 3.45	eyelid 3.25	forehead 2.75
		rank (percentage)	chin 4851 (2.14)	nose 30 (2.14)	glabella 61 (2.14)	**face shape 44 (13.59)**	lip 152 (13.59)	eye 197 (13.59)	eyelid 489 (13.59)	eyebrow 4211 (13.59)	philtrum 3583 (34.13)	forehead 2223 (34.13)
29		user study mean score	**nose 8.55**	eyebrow 8.05	eyelid 7.25	eye 6.15	face shape 5.65	lip 4.5	chin 4.05	glabella 3.8	philtrum 3.6	forehead 3.4
		rank (percentage)	eyelid 12 (0.13)	face shape 1 (0.13)	eyebrow 27 (2.14)	lip 120 (2.14)	**nose 128 (2.14)**	eye 4675 (13.59)	glabella 1149 (34.13)	philtrum 1266 (34.13)	chin 1489 (34.13)	forehead 2560 (34.13)
30		user study mean score	**eyebrow 8.85**	eye 8.0	glabella 7.85	lip 6.6	nose 6.3	forehead 5.0	face shape 3.7	eyelid 3.45	philtrum 3.3	chin 1.95
		rank (percentage)	glabella 4726 (13.59)	lip 4721 (13.59)	**eyebrow 4461 (13.59)**	eyelid 4545 (13.59)	eye 490 (13.59)	face shape 532 (13.59)	nose 652 (13.59)	philtrum 1258 (34.13)	forehead 2701 (34.13)	chin 2470 (34.13)

Figure 10. The results of the user study for the third 10 face images (21∼30). Dark orange cells denote components with a t-score falling in the 0.13% range, orange cells denote t-scores in the 2.14% range, and light orange cells indicate t-scores in the 13.59% range.

6.1.2. Analysis of the First User Study

We executed two analyses is to determine whether the dominant components from the xFoF ranking matched the components selected from the participants' rankings. In the first analysis, the dominant components recognized by the xFoF ranking percentages were compared to the results of the participants' rankings. Table 1 presents the results of how the participants ranked components in a range with t-score percentages of 0.13% (very dominant), 2.14% (dominant) and 13.59% (less dominant).

The table shows that the eight components belonging to the very dominant 0.13% percentage had an average ranking of 1.25 by the participants, with six components being ranked first and two being ranked second. The dominant 2.14% percentage included 42 components and had an average ranking of 1.80, with 20 components being ranked first, 14 being ranked second, 5 being ranked third and 2 being ranked fourth. The less dominant 13.59% percentage had an average ranking of 4.24. Based on the table, the components identified as dominant based on the xFoF ranking were also perceived as having high rankings by the participants in the user test.

Table 1. Participants' rankings for the dominant components that matched the xFoF ranking percentages.

xFoF Rank Percentage	Count	Participants' Ranking										
		1	2	3	4	5	6	7	8	9	10	Average
0.13%	8	6	2	0	0	0	0	0	0	0	0	1.25
2.14%	42	20	14	5	2	1	0	0	0	0	0	1.80
13.59%	118	4	14	25	26	21	15	9	4	0	0	4.24

The second analysis examined whether the components that the participants perceived as dominant had high xFoF rankings. Table 2 presents the xFoF ranking percentages for the participants' ranks. Specifically, this analysis presented the t-score percentages for the components that the participants ranked first, second and third. Among the components that the participants perceived as being first, there were 4 in the 0.13% range, 15 in the 2.14% range and 10 in the 13.59% range. For the components perceived as being second, there was 1 in the 0.13% range, 7 in the 2.14% range and 17 in the 13.59% range. Finally, for the components perceived as being third, there were 2 in the 0.13% range, 9 in the 2.14% range, and 14 in the 13.59% range. The analysis revealed that the components that the participants considered most important tended to be located in the lower xFoF ranking percentage ranges.

Table 2. The t-score percentages for the most dominant facial components selected by the participants.

Count	xFoF Rank Percentage				Total
	0.13%	2.14%	13.15%	Above 13.15%	
rank 1	4	15	10	1	30
rank 2	1	7	17	5	30
rank 3	2	9	14	5	30

6.2. Second User Study on Catching Overall Impressions

The primary goal of the second user study was to compare the perception of the overall impressions between the participants and xFoF-based approach. In this user study, a total of 30 participants were carefully selected to avoid any overlap with the individuals involved in the first user study. Of the participants, 14 were male and 16 were female, with 23 falling within the 20s age group and 7 being within the 30s age group. The user study encompassed an evaluation of 30 questions related to 20 faces, where the participants were instructed to assess each facial component using the five-point metric. Figure 11 illustrates the questions presented to the participants. Each question corresponded to a facial component and its morphological feature, which were assumed to comprise the overall impression of a face.

No	question	linear scale answer				
		1	2	3	4	5
1	eyes shape	eyes are thin				eyes are big and round
2	eyes width	short				long
3	corners of the eyes	eyes slanting downwards				eyes slanting upwards
4	eyes size	small				big
5	distance between eyebrows and eyes	short				long
6	glabella length	short				long
7	eyebrows width	short				long
8	corners of the eyebrow	eyebrows slanting downwards				eyebrows slanting upwards
10	eyebrows thickness	thin				thick
11	forehead height	short				long
12	philtrum height	short				long
13	chin height	short				long
14	chin width	short				long
15	square face shape	non square				square
16	circle face shape	non circle				circle
17	triangle face shape	non triangle				triangle
18	face height	short				long
19	face width	short				long
20	slender face shape	wide and round				narrow and slender
21	nose height	short				long
22	nose width	short				long
23	nose size	small				big
24	distance between nose tip and nostril	short				long
25	lip width	short				long
26	lip height	short				long
27	upper lip height	short				long
28	lower lip height	short				long
29	corners of the lip	lips slanting downwards				lips slanting downwards
30	lip size	small				big

No	question	multiple-choice answer			
9	eyebrow arch	inner	middle	outer	non eyebrows arch

Figure 11. The questions on facial impressions used in the second user study.

6.2.1. Catching Impressions Using a User Study

In this user study, the participants were requested to provide responses using a 5-point metric for 30 facial morphological features. Notably, the ninth feature utilized a four-point metric. These questions for the facial morphological features are presented in Figure 11. The scores gathered from the 30 participants were averaged to determine the overall user study score for each feature.

For the 20 target faces, Figure 12 illustrates the average scores and standard deviations derived from the assessments of the 30 features by the 30 participants. In this figure, each row corresponds to a question in Figure 11, and each column represents a test face. Each cell within the figure comprises two components: the upper component represents the mean, while the lower component indicates the standard deviation. Cells shaded in orange indicate a standard deviation value of 1 or higher, whereas dark orange cells indicate a value of 1.5 or higher. A question with a higher number of orange cells suggests a lack of consensus among the participants regarding that particular feature. Within each row, the light yellow items denote features where the standard deviation is 1.0 or higher for 5–10 out of the 20 faces, while the dark yellow items indicate features where the standard deviation is 1.0 or higher for more than 10 faces. Likewise, within each column, the blue items represent faces where the standard deviation is 1.0 or higher for 5–10 items.

Table 3 displays the distribution of standard deviations presented in Figure 12. A standard deviation of one or lower implies that the average difference in user responses was one or less, indicating consistent answers. Notably, the user scores with a standard deviation of 1 or lower amounted to 503 out of the total 580 scores, accounting for 86.7% of the scores. This observation suggests a significant level of consistency in 86.7% of the user responses.

Table 3. The count of answers in standard deviation categories.

Category of Standard Deviation	Count
0∼0.5	70
0.5∼1	433
1∼1.5	74
1.5∼2	3
total	580

In this figure, it is notable that only the 16th question exhibited a standard deviation of one or higher in more than 10 faces. Additionally, there were seven questions where the standard deviation fell within the range of 5–10. Considering this perspective, it becomes evident that 21 out of the 29 features demonstrated a consistent convergence of user opinions. Furthermore, upon examining the faces, there were six faces where five or more features showed a standard deviation difference of one or higher. Consequently, it can be concluded that out of the 20 faces, 14 exhibited a consistent convergence of user opinions.

6.2.2. Catching Impressions Using xFoFs

Five intervals were extracted from the xFoF ranking percentages for each facial component. In the case of components composed of multiple xFoFs, the corresponding xFoFs were averaged to determine the component's score. Figure 13 provides an overview of the associated xFoFs for each facial component. It is worth noting that the eye shape exhibited six corresponding xFoFs, setting it apart from the others where 1∼2 xFoFs were prevalent. Figure 13 showcases the scores computed based on xFoF ranking percentages.

	face																			
	1	**2**	**3**	**4**	**5**	**6**	**7**	**8**	**9**	**10**	**11**	**12**	**13**	**14**	**15**	**16**	**17**	**18**	**19**	**20**
1	1.58	4.42	4.33	2.67	1.67	3.67	4.22	2.00	4.56	2.56	4.38	4.00	4.50	2.25	4.63	4.00	4.50	3.63	3.88	2.50
	0.51	0.51	0.49	0.49	0.65	0.87	0.44	0.87	0.53	0.88	0.52	0.00	0.53	0.71	0.52	0.53	0.53	0.74	0.83	0.76
2	3.67	3.17	3.00	3.33	1.75	3.33	4.00	3.33	3.22	3.67	4.50	4.25	3.38	2.50	4.88	3.13	3.00	4.13	3.13	4.50
	0.78	0.72	0.85	0.78	0.75	1.12	0.71	0.71	1.09	0.50	0.76	0.89	0.92	1.20	0.35	0.83	1.31	0.83	1.13	0.53
3	2.67	3.67	3.08	2.50	2.50	2.11	2.00	2.11	4.56	2.67	4.13	2.25	2.63	2.00	3.88	1.50	3.00	1.25	3.75	1.75
	0.98	0.49	0.67	0.80	1.24	0.93	0.87	1.05	0.53	1.12	1.13	0.89	0.92	0.76	0.83	0.53	0.53	0.46	1.28	0.46
4	1.58	4.33	3.92	2.92	1.17	3.78	4.00	2.00	4.33	2.44	4.63	4.25	4.50	2.13	4.63	3.88	4.13	3.75	3.88	3.63
	0.51	0.78	1.00	0.79	0.39	0.67	0.50	0.87	0.50	0.53	0.52	0.46	0.53	0.99	0.52	0.99	0.64	0.89	0.83	1.06
5	4.17	2.25	1.92	2.92	4.08	3.11	1.22	3.00	3.11	2.89	1.50	1.75	3.38	2.63	1.00	2.25	1.13	2.50	4.50	2.38
	0.58	0.62	0.67	1.24	0.51	0.78	0.44	0.71	0.60	0.60	0.53	0.46	0.74	0.74	0.00	0.71	0.35	0.53	0.76	1.06
6	3.58	3.25	2.08	4.33	3.00	2.56	2.89	3.44	2.78	2.11	2.88	3.75	2.50	3.75	2.88	2.88	2.00	3.25	4.25	2.88
	1.08	0.45	0.67	0.65	0.43	0.73	0.93	0.88	0.67	0.78	0.99	0.89	0.93	0.46	0.64	0.64	0.53	1.39	0.71	0.83
7	3.42	3.75	2.25	2.33	3.92	2.22	4.67	2.56	4.11	4.33	4.88	4.25	4.50	3.00	4.88	3.88	4.50	4.25	4.88	3.25
	1.00	0.75	1.06	0.98	0.79	0.83	0.71	1.01	0.78	0.71	0.35	0.89	0.76	0.93	0.35	0.64	0.76	0.46	0.35	0.71
8	2.42	3.75	2.75	2.75	4.42	4.33	3.22	1.33	4.56	1.00	4.63	3.75	2.63	2.38	4.25	1.88	3.00	2.88	2.38	2.88
	0.90	0.97	0.75	0.45	0.67	0.71	0.44	0.50	0.53	0.00	0.52	1.16	1.77	0.74	0.46	0.83	0.00	0.99	1.92	0.35
10	3.42	2.83	3.75	3.75	2.00	3.67	4.78	1.22	1.44	3.67	2.13	4.25	4.50	3.25	3.63	2.63	3.13	2.75	1.00	4.75
	0.79	0.72	0.75	0.75	0.60	0.71	0.44	0.44	0.53	0.87	0.64	0.71	0.53	0.89	1.19	1.19	1.25	0.89	0.00	0.46
11	3.50	3.58	4.25	4.50	3.17	4.33	3.67	2.89	3.67	4.00	4.38	4.00	3.88	2.75	3.75	3.63	4.63	3.63	3.25	4.00
	1.17	0.51	0.97	0.67	0.94	0.50	1.12	1.17	1.00	1.00	0.52	1.07	0.99	0.89	0.71	0.92	0.52	0.74	1.28	0.76
12	2.17	2.83	2.92	2.33	2.75	4.00	3.67	1.56	2.89	2.67	2.63	2.88	4.00	3.75	1.75	3.88	3.88	2.25	3.38	2.25
	0.58	0.72	0.90	0.78	0.75	0.00	0.71	0.53	0.60	0.87	0.92	0.64	0.53	0.71	0.71	0.64	0.35	0.46	0.74	0.46
13	3.25	2.83	2.58	2.17	3.08	3.11	3.33	3.00	3.33	4.00	2.75	3.25	3.13	2.63	2.88	3.00	3.75	3.63	2.88	3.88
	0.87	0.83	0.90	0.72	0.51	0.78	0.87	0.71	0.71	0.50	0.71	0.89	0.64	0.92	0.83	0.76	0.71	0.74	0.64	0.83
14	3.25	2.08	2.42	4.58	3.42	4.00	1.89	3.78	2.67	4.44	2.63	1.50	1.88	4.38	3.50	3.75	3.00	4.13	3.63	4.00
	0.62	0.79	1.00	0.67	0.90	0.71	0.60	0.67	0.71	0.53	1.06	0.76	0.83	0.74	0.93	0.89	0.93	0.64	0.52	0.76
15	2.83	1.25	1.83	4.92	3.83	3.89	1.11	3.22	2.78	4.56	3.38	1.13	2.50	3.75	3.50	4.25	3.13	4.38	4.13	4.38
	0.94	0.62	0.83	0.29	0.58	0.60	0.33	1.09	1.09	0.53	0.74	0.35	1.20	1.28	1.20	0.46	1.13	0.52	0.35	0.52
16	3.25	1.92	2.58	2.25	2.83	3.56	1.33	3.89	2.33	3.33	1.63	1.88	2.38	4.50	3.00	3.50	2.13	2.75	3.13	2.63
	0.97	1.00	1.08	1.29	1.03	0.73	0.50	1.45	1.22	1.66	0.74	1.36	1.41	0.76	1.20	1.20	1.36	1.49	1.25	1.19
17	2.67	4.42	3.92	1.33	2.67	2.22	4.44	2.56	3.33	1.44	3.25	4.75	4.13	1.50	2.88	1.75	3.75	2.13	2.13	2.13
	0.98	0.67	0.79	0.65	1.15	1.09	0.73	1.42	1.00	0.73	0.89	0.46	0.35	0.76	1.36	1.04	1.16	1.13	1.13	1.25
18	3.00	3.42	3.00	2.67	2.75	3.22	4.00	2.78	3.67	3.33	4.00	4.00	3.25	2.50	3.38	3.00	3.75	3.25	3.50	3.88
	0.60	0.90	0.74	0.89	0.75	0.67	0.87	0.97	0.71	1.00	0.53	0.93	1.04	0.93	0.92	0.53	0.89	0.71	0.53	0.83
19	3.58	2.17	2.83	4.58	3.50	3.89	2.22	4.22	3.00	4.33	2.63	2.38	3.00	4.50	3.13	3.38	3.50	3.38	3.25	3.00
	0.51	0.72	0.83	0.51	0.80	0.78	0.83	0.97	0.87	1.32	0.92	0.92	0.76	0.53	0.83	0.92	0.53	0.52	0.71	0.76
20	2.17	4.42	3.67	1.50	2.33	2.33	4.56	1.67	3.22	1.11	3.75	4.75	3.75	1.13	2.88	1.88	3.00	2.75	2.38	3.00
	0.58	0.90	0.98	1.17	0.98	1.22	1.01	0.71	1.09	0.33	0.89	0.46	1.04	0.35	0.83	0.64	0.93	1.04	1.06	0.93
21	2.92	3.83	4.00	2.08	3.00	2.56	3.89	3.00	4.00	3.67	3.88	3.63	3.63	3.38	4.13	2.50	2.50	3.50	3.50	3.13
	1.00	0.83	0.43	0.79	0.43	0.73	0.33	0.50	0.50	0.50	0.35	0.74	0.92	1.06	0.64	0.76	0.93	0.53	0.93	0.83
22	3.58	2.33	2.50	4.58	2.75	3.22	1.89	3.89	2.78	2.89	2.13	3.13	2.00	3.25	3.50	3.00	3.00	2.38	2.25	3.88
	0.79	0.65	0.80	0.67	0.62	0.67	0.78	0.60	0.97	0.60	0.64	0.83	0.76	1.04	0.93	0.76	0.76	0.52	0.71	0.35
23	3.50	2.92	3.00	4.67	2.75	3.44	3.22	3.67	3.44	3.44	3.13	4.00	2.75	3.75	4.38	3.13	3.13	3.13	3.13	3.75
	0.67	0.67	0.60	0.65	0.45	0.73	0.67	0.71	0.53	0.88	0.64	0.53	0.71	1.04	0.52	0.99	0.64	0.64	0.64	0.71
24	2.25	2.33	2.67	4.67	3.33	2.56	2.78	3.33	1.00	2.78	1.38	1.63	2.88	4.13	1.38	4.50	4.38	2.88	4.13	4.38
	0.45	0.89	0.78	0.65	0.78	0.73	0.97	1.41	0.00	0.83	0.52	0.74	0.64	0.99	0.52	0.53	0.52	1.13	0.83	0.74
25	2.75	2.92	2.67	4.00	3.17	3.33	3.44	3.56	3.67	2.67	3.75	4.13	4.25	2.38	4.13	3.13	3.88	3.50	4.38	3.88
	0.75	0.79	0.65	0.74	0.58	0.50	0.73	0.88	0.71	0.50	0.46	0.64	0.71	0.92	0.99	0.64	0.83	0.93	0.52	0.64
26	4.00	3.33	2.25	3.08	2.67	3.00	3.00	4.67	3.00	2.00	3.63	2.88	3.75	2.13	4.63	2.38	1.50	3.38	4.13	4.13
	0.60	0.78	0.62	0.67	0.49	0.87	0.71	0.71	0.50	0.87	0.92	0.99	0.89	0.99	0.52	0.74	0.53	0.92	0.35	0.64
27	3.42	2.67	2.17	3.58	2.50	1.78	1.78	4.78	2.33	2.11	2.25	1.75	2.38	1.38	4.13	2.00	1.63	2.75	3.75	4.13
	1.00	0.98	0.58	0.79	0.52	0.67	0.44	0.44	0.71	1.36	1.04	0.71	0.92	0.52	0.64	0.76	0.52	1.04	0.71	0.64
28	4.25	3.33	2.50	2.75	2.75	3.67	3.44	3.89	3.33	1.67	4.00	3.75	4.13	2.38	4.63	2.13	1.75	3.75	3.88	3.13
	0.75	0.65	0.90	0.75	0.45	0.87	0.73	0.60	0.71	0.71	0.53	1.39	0.83	0.92	0.52	0.83	0.46	0.46	0.64	0.83
29	3.08	4.25	3.00	1.42	3.08	2.89	4.22	1.89	4.78	2.00	3.50	3.88	4.00	1.00	4.50	2.38	3.75	4.00	4.25	3.63
	1.00	0.45	0.43	0.51	0.67	0.93	0.67	0.60	0.44	0.71	0.53	0.64	0.53	0.00	0.76	0.92	0.89	0.76	0.46	0.74
30	3.92	3.00	2.33	3.58	3.00	3.11	3.44	4.44	3.44	2.11	3.75	3.50	3.75	1.75	4.75	2.38	2.13	3.38	4.13	3.75
	0.51	0.74	0.78	0.90	0.60	0.60	0.53	0.53	0.73	0.78	0.71	0.76	0.46	0.71	0.46	0.74	0.64	1.06	0.35	0.46

Figure 12. The results of the second user study. Cells shaded in orange indicate a standard deviation value of 1 or higher, whereas dark orange cells indicate a value of 1.5 or higher. Within each row, the light yellow items denote features where the standard deviation is 1.0 or higher for 5–10 out of the 20 faces, while the dark yellow items indicate features where the standard deviation is 1.0 or higher for more than 10 faces. Likewise, within each column, the blue items represent faces where the standard deviation is 1.0 or higher for 5–10 items.

No.	question	matching xFoF	faces																			
			1	2	3	4	5	6	7	8	9	10	11	12	13	14	15	16	17	18	19	20
1	eye shape	10, 11, 13, 14, 15, 16	2.2	4	3.2	2.2	2	3	3	2.2	3.2	3	3.2	3	3.7	2.2	3.5	3.2	4.2	3.3	3	2.7
2	eye width	9	3	3	3	3	2	3	3	3	3	3	4	3	4	3	5	3	4	4	4	4
3	corners of the eyes	12	3	4	3	3	3	3	3	3	5	3	3	3	3	2	3	1	2	2	2	2
4	eye size	17	3	4	3	2	2	3	3	3	3	3	4	3	4	2	4	3	4	3	3	3
5	distance between e yebrows and eyes	34	5	3	3	3	3	3	3	3	3	3	1	2	3	3	2	3	2	3	4	3
6	glabella length	35	5	3	3	3	3	2	3	3	3	2	3	4	2	2	3	3	2	2	3	3
7	eyebrows width	7	3	3	3	3	3	2	3	2	3	3	3	3	3	2	4	3	4	3	1	3
8	corners of the eyeb row	5	2	3	3	2	3	3	3	2	4	2	3	3	3	1	3	2	2	2	3	2
10	eyebrows thickness	8	3	3	3	2	3	2	4	2	3	3	3	3	3	3	3	3	3	3	2	4
11	forehead height	30	3	3	3	4	3	3	3	2	4	3	3	3	3	1	3	2	3	3	2	2
12	philtrum height	31	2	3	3	3	3	4	3	1	3	3	3	3	3	4	2	3	5	3	3	3
13	chin height	33	3	3	3	4	3	3	3	3	3	4	3	3	3	3	3	3	3	3	3	3
14	chin width	32	3	2	3	3	3	3	2	3	2	3	3	1	3	3	3	3	3	3	3	3
15	square face shape	3, 4	3	2.7	3	3.3	3	3	2.7	3	3	3	3	2.7	3	3	3	3	3	3	3	3
16	circle face shape	3, 4	4.3	3.7	4.3	3.7	4.3	4.3	3.7	4.3	4.3	4.3	4.3	3.7	4.3	4.3	4.3	4.3	4.3	4.3	4.3	4.3
17	triangle face shape	3, 4	3	3.3	3	2.7	3	3	3.33	3	3	3	3	3.3	3	3	3	3	3	3	3	3
18	face height	2	3	3	3	5	4	3	3	3	3	3	2	2	2	3	3	3	3	3	3	2
19	face width	1	3	2	3	4	3	4	2	3	2	3	2	1	2	3	3	3	3	3	2	3
20	slender face shape	2, 3, 4	3	4	3.6	2.5	3	3	3.9	3	4.5	2.9	4.3	4.8	3.1	3	3.5	2.1	3	3	3	3
21	nose height	18, 20	3	3	3	2	2	2	3	3	3	3	3	4	3	3	4	3	2	3	3	3
22	nose width	19, 20	3	2	2	4	2	2	2	3	2	3	2	3	2	2	3	2	2	2	1	3
23	nose size	22	3	3	3	3	3	1	3	4	3	2	3	3	2	3	3	2	2	2	3	3
24	distance between n ose tip and nostril	21	3	2	3	3	3	3	3	3	2	3	2	2	3	3	2	4	4	3	4	4
25	lip width	23, 27	3	3	2	3	3	3	3	3	3	2	3	3	3	2	4	3	3	3	4	3
26	lip height	24, 27	3	3	3	3	3	3	3	5	3	3	3	3	3	3	3	3	3	3	4	3
27	upper lip height	25	4	3	3	3	3	3	3	5	3	3	3	3	3	3	3	3	3	3	3	3
28	lower lip height	26	3	3	3	2	3	3	4	4	3	2	3	3	4	3	3	3	3	3	2	3
29	corners of the lip	28	2	3	3	2	3	3	3	2	4	2	3	3	3	1	3	2	2	2	3	2
30	lip size	29	3	4	3	3	3	3	3	4	3	2	3	3	3	3	5	3	2	3	5	3

Figure 13. The xFoF score, showing the score of the facial components from the xFoF ranking percentage.

6.2.3. Comparison of Impressions Caught by Both Methods

We compared the distributions of user scores obtained from the human participants in the second user study as depicted in Figure 12 with the distribution of xFoF scores presented in Figure 13. We analyzed the distributions of scores for both the components and the faces. As assuming normal distributions may be challenging, we conducted statistical tests including the Wilcoxon rank-sum test and Mann–Whitney U test to compare the distributions.

Analysis of the Faces

The results of the two tests conducted on each face are illustrated in Figure 14. This figure presents the p-values associated with each face, where a p-value exceeding 0.05 indicates the absence of a substantial distinction between the user score and xFoF rank score, as verified within a 99% confidence interval. Similarly, a p-value surpassing 0.01 suggests no noteworthy difference between the two scores at a 95% confidence interval. By employing the Wilcoxon rank-sum test, it was determined that there was no significant difference at a 99% confidence interval for 16 out of the total of 20 faces, while no significant difference was observed at a 95% confidence interval for 3 out of the total of 20 faces. Application of the Mann–Whitney U test yielded identical results. Consequently, there existed no considerable disparity between the user study-based scores and xFoF ranking-based scores for 19 out of the total of 20 faces.

face	p-values	
	Wilcoxon rank-sum test	Mann-Whitney U test
1	0.38	0.37
2	0.78	0.782
3	0.083	0.067
4	0.56	0.562
5	0.816	0.814
6	0.023	0.02
7	0.166	0.158
8	0.907	0.912
9	0.243	0.237
10	0.981	0.987
11	0.122	0.117
12	0.061	0.058
13	0.092	0.087
14	0.646	0.647
15	0.064	0.061
16	0.499	0.491
17	0.335	0.329
18	0.047	0.043
19	0.008	0.008
20	0.022	0.019
p >= 0.05	16 (80.0%)	16 (80.0%)
0.05 > P >= 0.01	3 (15.0%)	3 (15.0%)
0.01 > p	1 (5.0%)	1 (5.0%)

Figure 14. Wilcoxon rank-sum test and Mann–Whitney U test for the distributions of user scores and xFoF rank scores for the faces, where 16 out of 20 faces satisfy $p \geq 0.05$ and 19 out of 20 satisfy $p \geq 0.01$. Red figures denote p value is greater than 0.05, blue figures denote p values in (0.05, 0.01) and black denote p values smaller than 0.01.

Analysis of Features

The results of conducting these two tests for each component are presented in Figure 15. This figure displays the p-value for each component, where a p-value greater than 0.05 indicates no significant difference between the user score and xFoF rank score for that particular component, as verified within a 99% confidence interval. Similarly, a p-value greater than

0.01 indicates no significant difference between the two scores at a 95% confidence interval. In this study, the Wilcoxon rank-sum test revealed no significant difference at a 99% confidence interval for 18 out of 29 features and no significant difference at a 95% confidence interval for 6 out of 29 features. The Mann–Whitney U test yielded similar results. The Mann–Whitney U test revealed no significant difference at a 99% confidence interval for 17 out of 29 features and no significant difference at a 95% confidence interval for 7 out of 29 features. Consequently, according to this validation method, there was no significant difference between the user study-based scores and xFoF ranking-based scores for 24 out of the total of 29 features.

Facial component	p-value	
	Wilcoxon rank-sum test	Mann whitney U test
1	0.057	0.058
2	0.130	0.124
3	0.589	0.590
4	0.117	0.114
5	0.229	0.221
6	0.570	0.571
7	0.002	0.001
8	0.218	0.217
10	0.256	0.251
11	0.000	0.000
12	0.234	0.229
13	0.646	0.633
14	0.055	0.047
15	0.083	0.076
16	0.000	0.000
17	0.256	0.246
18	0.022	0.018
19	0.009	0.008
20	0.094	0.093
21	0.030	0.026
22	0.009	0.008
23	0.000	0.000
24	0.829	0.837
25	0.011	0.009
26	0.756	0.748
27	0.016	0.012
28	0.208	0.203
29	0.012	0.011
30	0.279	0.269
p >= 0.05	18 (62.1%)	17 (58.7%)
0.05 > P >= 0.01	6 (20.7%)	7 (24.1%)
0.01 > p	5 (17.2%)	5 (17.2%)

Figure 15. Wilcoxon rank-sum test and Mann–Whitney U test results for the distribution of user scores and xFoF rank scores for facial components, where 16 out of 20 faces satisfy $p \geq 0.05$ and 19 out of 20 satisfy $p \geq 0.01$. Red figures denote p value is greater than 0.05, blue figures denote p values in (0.05, 0.01) and black denote p values smaller than 0.01.

6.3. Discussion

In the first user study, we proved that the xFoF-based approach could catch the dominant impression perceived by a person. Through Tables 1 and 2, we showed that the facial components which were estimated to be very distinctive with the xFoF-based approach were also perceived by the participants, and vise versa. In the second user study, we proved that the xFoF-based approach could estimate the overall impressions perceived by a person. We applied the Wilcoxon rank-sum test and Mann–Whitney U test for the results from both the xFoF-based approach and the participants' evaluations and proved the similarity of the results for both the faces and features in Figures 14 and 15.

6.4. Limitations

The primary limitation of our study comes from the face landmark alignment and face segmentation scheme, since an xFoF is defined by the landmarks and segmented regions on faces. Facial features such as pupils and wrinkles that are not identified by the landmarks and regions are excluded in the xFoF definition. Many important features such as hair styles, mustaches and eyeglasses are not considered in xFoFs, since they are not captured through landmarks and segmentations. Another limitation comes from the dataset we employed in this study. Since our dataset comprised only Asian and Caucasian faces, the facial features from other ethnicities such as African Americans or Indians were not considered in estimating the xFoF rankings.

7. Conclusions and Future Studies

In this study, we defined the explicit features of faces (xFoFs) to estimate the facial impression perceived by a person. The xFoF is designed based on the anthropometry studies and defined by facial landmarks and segmented regions. The rankings of xFoFs for faces in a dataset were estimated to measure the human perception of facial impressions. We executed two user studies to examine our approach. The first user study proved that the dominant impressions perceived by a person and the xFoF-based method were similar. The second user study proved that the overall impressions of a human face perceived by a person and the xFoF-based method showed similar distributions.

We are going to apply the xFoF-based method for caption generation to human faces. This study will help disabled people to recognized human faces. Another direction is to apply our approach for a generative model that can control and explain the process of producing human faces or character faces.

Author Contributions: Conceptualization, J.L.; Methodology, J.Y.; Validation, H.Y.; Writing— original draft, K.M. All authors have read and agreed to the published version of the manuscript.

Funding: This research was supported by Sangmyung University at 2021.

Data Availability Statement: Not available.

Conflicts of Interest: The authors declare no conflict of interest.

Appendix A

We list the facial features suggested in various anthropometry studies [4,6,7,9–15,18,19,23,25,28,33] in Figure A1.

No.	feature	summary	reference
1	$d(27,62)$	intercanthal face height	[Merler2019]
2	$d(19,41)$	orbit and brow height (left)	
3	$d(24,46)$	orbit and brow height (right)	
4	$d(30,33)$	columella length	
5	$d(57,62)$	lower vermilion height	
6	$d(50,52)$	philtrum width	
7	$d(32,51)$	lateral upper lip height (left)	
8	$d(34,51)$	lateral upper lip height (right)	
9	$d(36,45)$	orbits biocular width	
10	$d(48,51)$	labio-oral region	
11	$\frac{d(27,8)}{d(2,14)}$	facial index	
12	$\frac{d(36,39)}{d(39,42)}$	orbital width index (left)	
13	$\frac{d(42,45)}{d(39,42)}$	orbital width index (right)	
14	$\frac{d(38,41)}{d(36,39)}$	eye fissure index (left)	
15	$\frac{d(43,46)}{d(42,45)}$	eye fissure index (right)	
16	$\frac{d(51,62)}{d(57,62)}$	vermilion height index	
17	$\frac{d(48,54)}{d(2,14)}$	mouth-face width index	
18	$d(3,13)$	cheek width	[Xie2015]
19	$d(4,12)$	cheek width	
20	$d(17,36)$	distance between eye and eyebrow(left)	
21	$d(26,45)$	distance between eye and eyebrow(right)	
22	$\frac{d(17,26)}{d(0,16)}$	eyebrows width	[Chen2021]
23	$\frac{d(36,39)+d(42,45)}{2*d(0,16)}$	eye width	
24	$\frac{d(41,47)}{d(0,16)}$	pupillary distance	
25	$\frac{2*d(27,33)}{d(21,8)\ +\ d(22,8)}$	nose height	
26	$\frac{d(50,52)\ +\ d(48,54)\ +\ d(58,56))}{3*d(3,13)}$	lip width	
27	$\frac{d(39{,}42)}{\left(d(36,39)+d(42,45)\right)/2}$	distance of glabella	[Alzahrani2021]
28	$angle(\overline{39,42},\overline{36,39})$	eye angles (left)	
29	$angle(\overline{39,42},\overline{42,45})$	eye angles (right)	
30	$\frac{d(0,16)}{d(8,68)}$	face width	[Sunhem2016]
31	$\frac{d(4,12)}{d(0,16)}$	chin width	
32	$\frac{d(8,57)}{d(4,12)}$	chin height	
33	$\frac{angle(i,8)+angle(j,8)}{2}$, $i=(0,1,2,\ldots,7)$, $j=(16,15,14,\ldots,9)$	face angles	

Figure A1. *Cont.*

No.	feature	summary	reference
34	$\frac{d(27,33)}{d(8,27)}$	naso-facial index	[Verma2021, Verma2022]
35	$\frac{d(51,57)}{d(48,54)}$	lip index	
36	$\frac{d(51,62)+d(51,66)}{d(8,27)}$	upper lip height	
37	$\frac{d(57,62)+d(57,66)}{d(8,27)}$	lower lip height	
38	$\frac{d(48,54)}{d(36,45)}$	lip width index	
39	$\frac{d(8,57)}{d(8,27)}$	chin size	
40	$\frac{d(8,27)}{d(1,15)}$	facial index	
41	$\frac{d(31,35)}{d(27,30)}$	nasal index	[Verma2022]
42	$\frac{d(31,35)}{d(1,15)}$	naso-facial width index	
43	$\frac{d(51,57)}{d(8,27)}$	lip height index	
44	$d(38,41)$	eye fissure height (left)	[Merler2019, Alrubaish2020 , Sezgin2023]
45	$d(43,46)$	eye fissure height (right)	
46	$d(2,14)$	face width	[Merler2019, Xie2015]
47	$d(5,11)$	face width	[Merler2019, Xie2015]
48	$d(36,39)$	orbits fissure length (left)	[Vegter2000, Merler2019, Kukharev2020, Alrubaish2020, Xie2015, Porter2001]
49	$d(42,45)$	orbits fissure length (right)	
50	$\frac{d(31,35)}{d(27,33)}$	nasal index	[Merler2019, Alrubaish2020]
51	$\frac{d(8,62)}{d(5,11)}$	mandibular index	[Merler2019, Kukharev2020]
52	$angle(\overline{17,21}) + angle(\overline{22,26})$	eyebrows angles	[Packiriswamy2013]
53	$d(33,62)$	upper lip height	[Vegter2000, Merler2019, Xie2015]
54	$d(27,68)$	head height	[Vegter2000, Merler2019, Xie2015, Porter2001]
55	$d(8,68)$	face height	[Merler2019, Ramanathan2006]
56	$d(8,27)$	face height	[Merler2019, Alsawwaf2022]
57	$d(8,33)$	face height	[Vegter2000, Merler2019, Xie2015]
58	$d(39,42)$	orbits intercanthal (width)	[Merler2019, Kukharev2020, Alsawwaf2022, Ramanathan2006, Xie2015, Zheng2022, Porter2001]
59	$d(27,33)$	nose height	[Vegter2000, Merler2019, Kukharev2020, Ramanathan2006, Xie2015, Zheng2022, Porter2001]
60	$d(31,35)$	nose width	[Merler2019, Kukharev2020, Alrubaish2020, Ramanathan2006, Xie2015, Zheng2022, Porter2001]
61	$d(6,10)$	chin width	[Alrubaish2020, Xie2015]
62	$d\ between\ pupils$	distance between pupils	
63	$d(0,16)$	face width	[Alrubaish2020, Alsawwaf2022, Ramanathan2006, Porter2001]
64	$\frac{d(39,42)}{d(36,45)}$	intercanthal index	[Merler2019, Verma2021, Verma2022]
65	$\frac{d(31,35)}{d(0,16)}$	nose width	[Verma2021]
66	$d(48,54)$	lip width	[Vegter2000, Kukharev2020, Alrubaish2020, Xie2015, Porter2001]
67	$d(8,62)$	chin height	[Vegter2000, Xie2015]
68	$d(57,66)$	lower lip height	[Vegter2000]

Figure A1. Facial features in anthropometry studies.

References

1. Zhou, H.; Liu, J.; Liu, Z.; Liu, Y.; Wang, X. Rotate-and-render: Unsupervised photorealistic face rotation from single-view images. In Proceedings of the IEEE/CVF Conference on Computer Vision and Pattern Recognition (CVPR), Seattle, WA, USA, 14–19 June 2020; pp. 5911–5920.
2. Yu, C.; Gao, C.; Wang, J.; Yu, G.; Shen, C.; Sang, N. Bisenet v2: Bilateral network with guided aggregation for real-time semantic segmentation. *Int. J. Comput. Vis.* **2021**, *129*, 3051–3068. [CrossRef]
3. King, D.E. Dlib-ml: A machine learning toolkit. *J. Mach. Learn. Res.* **2009**, *10*, 1755–1758.
4. Farkas, L. *Anthropometry of the Head and Face*; Raven Press: New York, NY, USA, 1994.
5. Vegter, F.; Hage, J.J. Clinical anthropometry and canons of the face in historical perspective. *Plast. Reconstr. Surg.* **2000**, *106*, 1090–1096. [CrossRef] [PubMed]
6. Merler, M.; Ratha, N.; Feris, R.S.; Smith, J.R. Diversity in faces. *arXiv* **2019**, arXiv:1901.10436.
7. Kukharev, G.A.; Kaziyeva, N. Digital facial anthropometry: Application and implementation. *Pattern Recognit. Image Anal.* **2020**, *30*, 496–511. [CrossRef]
8. Szlávik, Z.; Szirányi, T. Face identification with CNN-UM. In Proceedings of the IEEE International Workshop on Cellular Neural Networks and their Applications(CNNA), Budapest, Hungary, 22–24 July 2004; pp. 190–195.
9. Alrubaish, H.A.; Zagrouba, R. The effects of facial expressions on face biometric system's reliability. *Information* **2020**, *11*, 485. [CrossRef]
10. Alsawwaf, M.; Chaczko, Z.; Kulbacki, M.; Sarathy, N. In your face: Person identification through ratios and distances between facial features. *Vietnam J. Comput. Sci.* **2022**, *9*, 187–202. [CrossRef]
11. Hong, Y.-J. Facial Identity Verification Robust to Pose Variations and Low Image Resolution: Image Comparison Based on Anatomical Facial Landmarks. *Electronics* **2022**, *11*, 1067. [CrossRef]
12. Ramanathan, N.; Chellappa, R. Modeling age progression in young faces. In Proceedings of the Computer Society Conference on Computer Vision and Pattern Recognition (CVPR'06), New York, NY, USA, 17–22 June 2006; pp. 387–394.
13. Sunhem, W.; Pasupa, K. An approach to face shape classification for hairstyle recommendation. In Proceedings of the Eighth International Conference on Advanced Computational Intelligence (ICACI), Chiang Mai, Thailand, 14–16 February 2016; pp. 390–394.
14. Alzahrani, T.; Al-Nuaimy, W.; Al-Bander, B. Integrated multi-model face shape and eye attributes identification for hair style and eyelashes recommendation. *Computation* **2021**, *9*, 54. [CrossRef]
15. Chen, Y.; Zhang, Y.; Huang, Z.; Luo, Z.; Chen, J. CelebHair: A new large-scale dataset for hairstyle recommendation based on CelebA. In Proceedings of the International Conference on Knowledge Science, Engineering and Management, Tokyo, Japan, 14 August 2021; pp. 323–336.
16. Liu, Y.; Schmidt, K.L.; Cohn, J. F.; Mitra, S. Facial asymmetry quantification for expression invariant human identification. *Comput. Vis. Image Underst.* **2003**, *91*, 138–159. [CrossRef]
17. Little, A. C.; Jones, B. C.; DeBruine L. M. Facial attractiveness: Evolutionary based research. *Philos. Trans. R. Soc. Biol. Sci.* **2011**, *366*, 1638–1659. [CrossRef]
18. Xie, D.; Liang, L.; Jin, L.; Xu, J.; Li, M. Scut-fbp: A benchmark dataset for facial beauty perception. In Proceedings of the IEEE International Conference on Systems, Man, and Cybernetics, Hong Kong, China, 9–12 October 2015; pp. 1821–1826.
19. Zheng, S.; Chen, K.; Lin, X.; Liu, S.; Han, J.; Wu, G. Quantitative analysis of facial proportions and facial attractiveness among Asians and Caucasians. *Math. Biosci. Eng.* **2022**, *19*, 6379–6395. [CrossRef] [PubMed]
20. Wei, W.; Ho, E.S.L.; McCay, K.D.; Damaševičius, R.; Maskeliūnas, R.; Esposito, A. Assessing facial symmetry and attractiveness using augmented reality. *Pattern Anal. Appl.* **2022**, *25*, 635–651. [CrossRef]
21. Roelofse, M.M.; Steyn, M.; Becker, P. J. Photo identification: Facial metrical and morphological features in South African males. *Forensic Sci. Int.* **2008**, *177*, 168–175. [CrossRef] [PubMed]
22. Moreton, R. Forensic face matching: Procedures and application. In *Forensic Face Matching: Research and Practice*; Bindemann, M., Ed.; Oxford University Press: Oxford, UK, 2021; pp. 144–173.
23. Verma, R.; Bhardwaj, N.; Singh, P. D.; Bhavsar, A.; Sharma, V. Estimation of sex through morphometric landmark indices in facial images with strength of evidence in logistic regression analysis. *Forensic Sci. Int. Rep.* **2021**, *4*, 100226. [CrossRef]
24. Sezgin, N.; Karadayi, B. Sex estimation from biometric face photos for forensic purposes. *Med. Sci. Law* **2023**, *63*, 105–113. [CrossRef]
25. Porter, J. P.; Olson K. L. Anthropometric facial analysis of the African American woman. *Arch. Fac. Plast. Surg.* **2001**, *3*, 191–197. [CrossRef]
26. Farkas, L.G.; Katic, M.J.; Forrest, C.R. International anthropometric study of facial morphology in various ethnic groups/races. *J. Craniofac. Surg.* **2005**, *16*, 615–646. [CrossRef]
27. Zhuang, Z.; Landsittel, D.; Benson, S.; Roberge, R.; Shaffer, R. Facial anthropometric differences among gender, ethnicity, and age groups. *Ann. Occup. Hyg.* **2018**, *54*, 391–402.
28. Packiriswamy, V.; Kumar, P.; Bashour, M. Photogrammetric analysis of eyebrow and upper eyelid dimensions in South Indians and Malaysian South Indians. *Aesthetic Surg. J.* **2013**, *33*, 975–982. [CrossRef]
29. Maalman R. S.-E.; Abaidoo, C.S.; Tetteh, J.; Darko, N.D.; Atuahene, O.O.-D.; Appiah, A.K.; Diby, T. Anthropometric study of facial morphology in two tribes of the upper west region of Ghana. *Int. J. Anat. Res.* **2017**, *5*, 4129–4135. [CrossRef]

30. Dancey, C.; Reidy, J. *Statistics without Maths for Psychology*; Pearson Education: New York, NY, USA, 2017.
31. Niu, Z.; Zhou, M.; Wang, L.; Gao, X.; Hua, G., Ordinal regression with multiple output CNN for age estimation. In Proceedings of the IEEE Conference on Computer Vision and Pattern Recognition (CVPR), Las Vegas, NV, USA, 27–30 June 2016; pp. 4920–4928.
32. Ward, A.; Murray-Ward, M. *Assessment in the Classroom*, 1st ed.; Wadsworth Pub.: Wadsworth, OH, USA, 1999.
33. Verma, R.; Bhardwaj, N.; Bhavsar, A.; Krishan, K. Towards facial recognition using likelihood ratio approach to facial landmark indices from images. *Forensic Sci. Int. Rep.* **2022**, *5*, 100254. [CrossRef]